ADA198049

20030130138

SECURITY CLASSIFICATION OF THIS PAGE

REPORT DOCUMENTATION PAGE

Form Approved OMB No. 0704-0188

1a. REPORT SECURITY CLASSIFICATION: Unclassified	1b. RESTRICTIVE MARKINGS
2a. SECURITY CLASSIFICATION AUTHORITY	3. DISTRIBUTION/AVAILABILITY OF REPORT: Approved for public release; distribution unlimited
2b. DECLASSIFICATION/DOWNGRADING SCHEDULE	
4. PERFORMING ORGANIZATION REPORT NUMBER(S)	5. MONITORING ORGANIZATION REPORT NUMBER(S)
6a. NAME OF PERFORMING ORGANIZATION: University of Maryland School of Medicine; 6b. OFFICE SYMBOL (If applicable)	7a. NAME OF MONITORING ORGANIZATION
6c. ADDRESS (City, State, and ZIP Code): Baltimore, MD 21201	7b. ADDRESS (City, State, and ZIP Code)
8a. NAME OF FUNDING/SPONSORING ORGANIZATION: U.S. Army Medical Research & Development Command; 8b. OFFICE SYMBOL (If applicable)	9. PROCUREMENT INSTRUMENT IDENTIFICATION NUMBER: DAMD17-84-C-4219
8c. ADDRESS (City, State, and ZIP Code): Fort Detrick, Frederick, Maryland 21701-5012	10. SOURCE OF FUNDING NUMBERS: PROGRAM ELEMENT NO. 61102A; PROJECT NO. 3M1-61102BS11; TASK NO. AA; WORK UNIT ACCESSION NO. 056

11. TITLE (Include Security Classification): The Molecular Targets of Selected Organophosphorus Compounds at Nicotinic, Muscarinic, GABA and Glutamate Synapses: Acute and Chronic Studies Including Prophylactic and Therapeutic Approaches

12. PERSONAL AUTHOR(S): Edson X. Albuquerque, M.D., Ph.D.

13a. TYPE OF REPORT	13b. TIME COVERED	14. DATE OF REPORT (Year, Month, Day)	15. PAGE COUNT
Annual Report	FROM 9/15/85 TO 9/14/86	1987 January 10	47

16. SUPPLEMENTARY NOTATION

17. COSATI CODES			18. SUBJECT TERMS (Continue on reverse if necessary and identify by block number)
FIELD	GROUP	SUB-GROUP	
06	15		cholinesterase, organophosphorus agents, acetylcholine, nicotinic receptor-ion channel complex, desensitization, oximes, irreversible cholinesterase inhibitors, oximes, (KT)
06	16		

19. ABSTRACT (Continue on reverse if necessary and identify by block number)

Studies during the past year have been focused on: a) continuing the investigation of the organophosphorus compounds (OPs) on the chemosensitive receptors located at various synapses; b) attempting to discern the active sites of the receptor-ion channel complexes involved in activation, desensitization and blockade; c) establishing the concentration gradients for various noncompetitive antagonists for production of states of activation, inactivation and blockade of the receptor-channel macromolecule; d) delineating avenues of testing, in in vivo and in vitro conditions, new agents which will be proven effective in alleviation of symptomatology and intoxication produced by OPs; e) recommending an agent or combination of agents which will be prophylactically and therapeutically effective against OP intoxication. (Keywords: organophosphates;)

20. DISTRIBUTION/AVAILABILITY OF ABSTRACT	21. ABSTRACT SECURITY CLASSIFICATION
☐ UNCLASSIFIED/UNLIMITED ☒ SAME AS RPT ☐ DTIC USERS	Unclassified

22a. NAME OF RESPONSIBLE INDIVIDUAL	22b. TELEPHONE (Include Area Code)	22c. OFFICE SYMBOL
Mrs. Virginia Miller	301/663-7325	SGRD-RMT-S

DD Form 1473, JUN 86 — Previous editions are obsolete. — SECURITY CLASSIFICATION OF THIS PAGE

18. electrophysiological investigations, agonists, neuromuscular junction

The Molecular Targets of Selected Organophosphorus Compounds at Nicotinic, Muscarinic, GABA, and Glutamate Synapses: Acute and Chronic Studies Including Prophylactic and Therapeutic Approaches

ANNUAL REPORT

September 15, 1985 - September 14, 1986

By Dr. E.X. Albuquerque

Supported by:

U.S. ARMY MEDICAL RESEARCH AND DEVELOPMENT COMMAND
Fort Detrick, Frederick, Maryland 21701-5012

Contract No. DAMD17-84-C-4219

University of Maryland
Baltimore, Maryland 21201

TABLE OF CONTENTS

A. SUMMARY:

Studies during the past year have been focused on: a) continuing the investigation of the organophosphorus compounds (OPs) on the chemosensitive receptors located at various synapses; b) attempting to discern the active sites of the receptor-ion channel complexes involved in activation, desensitization and blockade; c) establishing the concentration gradients for various noncompetitive antagonists for production of states of activation, inactivation and blockade of the receptor-channel macromolecule; d) delineating avenues of testing, in in vivo and in vitro conditions, new agents which will be proven effective in alleviation of symptomatology and intoxication produced by OPs; e) recommending an agent or combination of agents which will be prophylactically and therapeutically effective against OP intoxication.

B. FORWARD:

In conducting the research described in this report, the investigators adhered to the "Guide for the Care and Use of Laboratory Animals," prepared by the Committee on Care and Use of Laboratory Animals of the Institute of Laboratory Animal Resources, National Research Council (DHEW) Publication No. (NIH) 78-23, Revised 1978).

C. METHODOLOGY:

Electrophysiological techniques:

Tissue preparations, solutions and drugs. All data were collected at room temperature (20-22°C) from sartorius, cutaneous pectoris and 10°C from interosseal muscles of the frog, Rana pipiens, or from chronically denervated (7-14 days) soleus muscle of the Wistar rat (180-200 g). The physiological solution used for the frog muscles had the following millimolar composition: NaCl, 116; KCl, 2.0; $CaCl_2$, 1.8; Na_2HPO_4, 1.3; and NaH_2PO_4, 0.7. The frog Ringer's solution was bubbled with 100% O_2 and had a pH of 6.9-7.1. The physiological solution for mammalian muscle had the following millimolar composition: NaCl, 135; KCl, 5.0; $MgCl_2$, 1.0; $CaCl_2$, 2.0; $NaHCO_3$, 15.0; and Na_2HPO_4, 1.0. During experiments this solution was continuously aerated with 95% O_2/5% CO_2, and the pH was 7.1-7.2.

Twitch studies. Twitch studies were performed on frog sartorius muscle with sciatic nerve attached. Direct muscle stimulation was applied by platinum bipolar electrode, using supramaximal square-wave pulses of 2-3 msec duration. Indirect stimulation was applied via the sciatic nerve by a separate platinum bipolar electrode, using supramaximal square-wave pulses of 0.05-0.1 msec duration. Indirect stimulation volleys were applied at a frequency of 0.2 Hz. To study direct evoked muscle twitch, neuromuscular transmission was blocked by alpha-bungarotoxin (α-BGT) (5 μg/ml). In all experiments the sartorius muscle was allowed to equilibrate under stimulation for 20-30 min before addition of drug. For each drug concentration, the duration of exposure was chosen to allow maximal effects to be observed; the exposures ranged from 15 to 45 min with maximal effects usually occurring 10-20 min after the addition of a new drug concentration.

Endplate current analysis. Frog sartorius muscles with nerve attached were treated with 400-600 mM glycerol to disrupt excitation-contraction coupling. The voltage-clamp circuit was similar to that of Takeuchi and Takeuchi (1) as modified by Kuba et al. (2). The membrane voltage sequence for endplate current (EPC) experiments consisted of 10-mV conditioning steps made in both depolarizing and hyperpolarizing directions throughout the range of +60 to -160 mV. Occasionally, larger steps were used to check for hysteresis (for details see ref. 3). Each conditioning step was 3 sec in duration; at the end of each conditioning step, an EPC was elicited by nerve stimulation. The EPC waveforms were displayed on an oscilloscope and digitized at 10 kHz by a PDP 11/40 minicomputer (Digital Equipment Corporation, Maynard, Massachusetts). The rise times and peak amplitudes were obtained directly from the digitized EPC data. The decay phase (80%-20%) was fit by a single exponential (linear regression on the logarithms of the data points) from which the EPC decay time constant (τ_{EPC}) was determined.

Miniature EPC and EPC fluctuation (noise) analysis. For spontaneous miniature endplate current (MEPC) and EPC fluctuation experiments, the signals were sampled at the junctional region of surface fibers of the cutaneous pectoris muscles, using conventional techniques for recording and analysis (3-5). Unfiltered signals were recorded on an FM tape recorder (Racal 4DS, Vienna, Va.) and displayed on a Mingograf 81 chart recorder (frequency response dc-700 Hz). MEPCs were filtered (1-2500 Hz) by a bandpass filter (Krohn-Hite 3700, Avon, Ma.) and briefly stored in a digital oscilloscope (Gould OS4000, Greenbelt, Md.) before being transmitted to the PDP 11/40 computer for signal averaging and analysis. The acetylcholine (ACh)-induced noise was displayed as a low-gain dc trace on the Mingograf for mean current measurement and at high-gain on the FM tape recorder for current fluctuation measurement. The high-gain noise signal was filtered from 1-800 Hz and digitized at 2 kHz. After records containing either MEPCs or electrical artifacts were removed, a Fourier analysis was performed on 512-point samples. Each spectrum is the difference between the average of about 30 baseline and 30 ACh spectra. The power density spectrum of the noise was fit to a single Lorentzian function using a nonlinear regression program. The single-channel lifetime (τ_I) was obtained from the half-power frequency (f_c) of the Lorentzian curve ($\tau_I = 1/2\pi f_c$). The single-channel conductance (γ) was calculated using the expression:

$$\gamma = S(0) / 4\,\mu(V_m - V_{eq})\tau_I,$$

where μ is the mean dc current, V_m is the holding potential, $V_{eq} = -15$ mV is the equilibrium potential, and $S(0)$ is the zero-frequency asymptote.

Double-barrel ACh microiontophoresis. The details of this technique have been described previously (6). Both barrels of a double-barrel microiontophoretic pipette were filled with 2 M ACh. One barrel of the micropipette was used for microiontophoresis of a long (30 sec) conditioning charge to release ACh, while the other barrel was used to deliver repetitive (1 Hz) brief (50-100 μsec) charges. The position of the double-

barrel micropipette was adjusted so that the 50-μsec charges applied to the ACh pipette induced a response of <1.0 msec rise time. A single intracellular microelectrode measured the transient membrane depolarizations due to ACh. The decrease of ACh potential amplitudes delivered at 1 Hz during the conditioning pulse and the recovery time of the amplitudes after the end of the conditioning pulse are measures of desensitization.

Isolation of muscle fibers for patch clamping. Interosseal muscles were dissected from the longest toe of the hind foot of the frog Rana pipiens in standard Ringer's solution. The procedure for isolation of single fibers was reported previously (7). Briefly, the muscles were incubated in 1 mg/ml of collagenase (type I, Sigma Chemical Co., St. Louis, Mo.; 2 hr, 21°C) and then in 0.2 mg/ml of protease (type VII, Sigma; 12-20 min) with mild agitation. Fibers were stored in bovine serum albumin (0.3-0.5 mg/ml) and used within 24 hr. Tetrodotoxin (300 nM; Sigma Chemical Co., St. Louis, Mo.) was added to all solutions used in patch clamp studies to prevent contraction of the muscle fibers.

Patch clamp recording technique. Microelectrodes of borosilicate capillary glass were pulled in two stages and heat polished to yield micropipettes with resistance of 8-12 MΩ. ACh and/or test drugs were diluted in HEPES-buffered solution and filtered through a Millipore filter before filling the micropipette. The recording bath was filled with HEPES-buffered solution and maintained at 10°C. GigaΩ seals between the nonjunctional surface of the fiber membrane and the microelectrode were formed using standard technique (8). Patch clamp currents from cell-attached patches were monitored using an LM-EPC-7 instrument (List Electronic, Darmstadt, West Germany). The signal was filtered with a Bessel filter at 3 kHz and recorded on FM magnetic tape for later analysis.

For computer analysis, the signal was filtered at 3 kHz with a fourth order Bessel filter (low pass) and digitized at 0.08-msec intervals. Analysis was done by PDP 11/24 and PDP 11/40 computers (Digital Equipment Corp.) using a maximum zero-crossing algorithm to establish baselines and channel amplitudes (9). A channel opening was counted when the current was greater than 50% of the estimated average channel current. After an opening, the channel was considered to be closed when the current decreased to less than 50% of the mean channel current. Open events which occurred without interruption were analyzed for channel lifetime. When closures of less than 8 msec occurred between openings, the openings were considered to be part of a burst. The channel lifetime (τ) value was estimated using unweighted least-squares fitting of a single exponential function to the open time histograms. The histograms for closures less than 8 msec were fitted well by single exponential decays.

Tissue preparation for light microscopy. After experimental treatments, the rats were anesthetized with ether and soleus muscles from the left limb were removed. The slow twitch soleus muscle was selected for study because it has been reported to be more affected by sarin than fast twitch extensor digitorum longus muscles (10). The soleus muscles were pinned loosely on a sylgard plate and fixed immediately by immersion in 3% paraformaldehyde and 1% glutaraldehyde in 0.15 M cacodylate buffer (pH 7.2)

for 1 hr. The muscles were then washed and stored in a 0.15 M cacodylate buffer. Junctional regions were identified by reacting the whole muscle for cholinesterase (ChE) activity, using ACh iodide as the substrate (11). Identified endplate regions were cut into small pieces and the precipitate was removed by washing 2 to 3 days in 0.15 M cacodylate buffer. Blocks of tissues containing the motor endplate were postfixed in 1% osmium tetroxide, stained en bloc with 0.5% uranyl acetate, dehydrated and embedded in epon 812. Semithin plastic sections (1-1.5 μm) were cut from longitudinally oriented blocks and stained with toluidine blue to locate motor endplates. Ultrathin sections prepared from these blocks were stained with uranyl acetate and lead citrate and examined in a Zeiss EM 109 electron microscope.

Quantitative morphometry. Light-microscopic analysis of semithin plastic sections. For all drug treatment groups, the area, perimeter, width and length of myopathic lesions were determined using a video-camera-equipped microscope in which the image was projected onto a digitization pad (Bioquant system, Nashville, Tenn.). A planimeter program generated a running total of trapezoid areas swept by the cursor. All the measured data from each group were averaged and the standard error of the mean was calculated. The two-tailed Student's t-test was used for statistical comparison of the data. The difference between two mean values was considered significant if the probability value (P) was found to be < 0.05.

D. DETAILED REPORT:

Comparative study of the effects of organophosphorus compounds on frog neuromuscular transmission.

The primary cause of acute toxic effects of OPs has been attributed to their ability to inhibit the acetylcholinesterase (AChE) in an irreversible manner. Earlier studies from our laboratory and elsewhere indicate that both reversible and irreversible ChE inhibitors could affect targets other than AChE at the cholinergic synapses and may also modulate noncholinergic transmission. Since the neuromuscular synapse forms one of the key target sites of OP action, it is essential to understand how the molecular events underlying neurotransmission are altered by OPs in order to counter their toxic effects effectively. During the second year of this contract, we attempted to partially answer this problem by studying the neuromuscular effects of different OPs (soman, sarin, tabun and VX) at steps between release of neurotransmitter and the occurrence of single-channel current events.

Experiments were conducted using frog sciatic nerve-sartorius muscle preparations for recording of EPCs (Figures 1 and 2) and MEPCs (Figures 3, 4 and 5). Except for tabun, the other OPs at low concentrations (< 1 μM) facilitated, whereas high doses (> 10 μM) of all four depressed, the EPC peak amplitude, VX producing a greater depression. The time constant of EPC decay (τ_{EPC}) was prolonged, and a maximum increase was achieved with 1

μM in the case of VX, sarin and tabun whereas soman produced a maximal increase at a 0.1-μM concentration. Doses > 1 μM of all OPs shortened the τ_{EPC} from an enhanced level already achieved by a low dose. At the 1-μM concentration, all four OPs produced near-maximal enhancement (approximately 3 times greater than control) of the EPC decay time constant, whereas at doses of 10 μM and above, the τ_{EPC} values appeared lower than that observed with the 1-μM dose; again, a greater reduction was observed with VX. The enhancement of τ_{EPC} can be attributed to inhibition of AChE, whereas the reduction seen with higher doses appears to be due to their action on the acetylcholine receptor (AChR)-ion channel complex or to the associated ionic channels. The reduction in the τ_{EPC} seen with higher concentrations of VX (particularly at more negative holding potentials) is indicative of an open channel blocking action of the drug.

Each of the four OPs affected the MEPC parameters in a different fashion. The frequency of MEPCs was increased only by VX (Figure 3). MEPC peak amplitude was enhanced to a greater degree by low doses than by high doses of soman, sarin (Figure 4), and VX, whereas a dose-dependent enhancement was observed in the case of tabun (Figure 4). This discrepancy between the effects seen on peak amplitude of EPCs and MEPCs in the presence of these OPs would mean an involvement of a presynaptic component in their effects. By comparing the I-V plots of EPCs and MEPCs, it is possible to make some general predictions in that both VX and tabun could reduce the release of transmitter, whereas sarin might even enhance this release. Indeed our quantal content experiments with VX clearly indicate its efficacy to reduce the evoked ACh release. A change in the affinity of the receptors to ACh could be an alternate explanation for the above effects. Soman, sarin (Figure 5) and VX, at high concentrations (> 10 μM), caused a reduction of the time constant of MEPC decay (τ_{MEPC}) from the enhanced level produced by a low dose. On the other hand, tabun at high concentrations (> 10 μM) caused only a slight decrease in τ_{MEPC} (Figure 5).

The direct interactions of VX with the postsynaptic AChR were analyzed in more detail at the single-channel current level. Single-channel currents were recorded from frog interosseal muscle fibers (Figure 6). VX at concentrations ranging from 5 to 50 μM produced a concentration- and voltage-dependent shortening of the channel open times (Figures 7 and 8) without significant change of the channel conductance. Unlike neostigmine and edrophonium (12), VX induced well-separated short pulses with no clear bursting activity, indicating a relatively stable blocked state. The reduction in single-channel lifetime correlates well with the EPC results, confirming the hypothesis of an open channel blockade by VX. However, in the cases of sarin, soman and tabun, it is not clear whether the changes seen in the τ_{EPC} are a consequence of a similar channel-blocking effect and/or to a decrease in the availability of the AChR as usually seen in a desensitized state. Sarin, at least, does not appear to block the AChR channels (Figure 9).

In summary, the four OPs used in this study, though sharing the common effect of inhibiting AChE, appear to induce differential effects at the cholinergic synapse. The relevance of these effects to the toxic effects of these compounds can be exploited for finding better remedies to tackle

OP poisoning.

OP-oxime interactions in the rat phrenic nerve-diaphragm muscle preparation.

It is generally considered that the beneficial effects of oximes in OP poisoning are due to reactivation of phosphorylated AChE. To determine the contribution of enzyme reactivation and possible direct effects of oximes at the neruomuscular junction in reversing the depression of muscle function induced by OP agents, phrenic nerve-diaphragm muscle preparations of the rat were used and twitches (0.1 Hz) and tetani (20 and 50 Hz nerve stimulation for 4 sec duration) were recorded in control conditions, in the presence of soman or sarin, and after application of HI-6 (100 μM) or 2-PAM (upto 1 mM). HI-6 produced almost complete recovery (10-20 min) in both twitch and tetanic (50 Hz) depression induced by soman (0.1 and 0.2 μM) and sarin (0.2 and 0.4 μM). In contrast, 2-PAM was only effective against sarin and not against soman. Determination of AChE activity under all conditions is in progress. The recovery in muscle was maintained even after washing HI-6 or 2-PAM. It appears that depression and inability of skeletal muscles to sustain tetanus in the presence of OPs are most likely due to direct effects of OPs at the AChR. The effectiveness of HI-6 in reversing this depression could be through an action of this oxime at the AChR.

Effects of carbamates and OP agents on desensitization at the nicotinic AChR in mammalian soleus muscle.

Electrophysiological studies at the microscopic level with nerve agents soman, sarin and VX and carbamates pyridostigmine and physostigmine have shown these agents to act as agonists at the AChR with varying potency. Desensitization with a drug can be best studied by application of iontophoretic pulses of ACh (2 M) at 8-10 Hz in denervated (12-15 days) soleus muscles of rats. The muscles were removed from rats under ether anesthesia and perfused <u>in vitro</u> with physiological solution containing 1 μM tetrodotoxin to prevent spontaneous twitching. In control condition ACh potentials having rising phase < 1 msec were obtained by iontophoretic pulses (1 msec in duration) of ACh. After recording responses to 8 Hz trains in 3 fibers the procedure was repeated in the presence of varying concentrations of carbamate pyridostigmine or OP agents sarin, soman and VX. Only the trails in which responses to single stimuli recovered following the train were analyzed for determining the degree of desensitization. Effects of pyridostigmine and OP agents sarin and VX on desensitization in the soleus muscle are shown in Figure 10. At concentration $\geq$ 10 μM, these drugs showed 30-50% desensitization which recovered upon washing. Similar results were obtained with soman.

Recently, using forskolin, a specific adenylate cyclase activator, we and other investigators have demonstrated that the process of desensitization at the nicotinic AChR involves cyclic AMP-dependent phosphorylation (13-15). Preliminary experiments with sarin and pyridostigmine have shown that desensitization induced by these agents is enhanced in the presence of forskolin (1-5 μM). It is indeed likely that

desensitization induced by carbamates and nerve agents is mediated via second messengers such as cyclic AMP and protein kinase C.

Mechanisms of interaction of the oximes pralidoxime chloride and HI-6 with organophosphate-poisoned frog muscle.

Oximes such as pralidoxime chloride (2-PAM) have been considered as antidotal agents in OP poisoning because of their ability to reactivate the phosphorylated AChE enzyme. Early studies by Kuba et al. (2) have indicated a direct effect of the oxime 2-PAM on the nicotinic AChR. In order to gain more insight into their mechanisms of action, the oximes 2-PAM and HI-6 were tested on the EPCs recorded from frog sartorius muscle in the absence and presence of either irreversible (soman, sarin, tabun or VX) or reversible (physostigmine) AChE inhibitors. EPCs were recorded from the frog sciatic nerve-sartorius muscle preparations. Results obtained from EPC analysis with 2-PAM alone disclosed two distinct effects: 1) a facilitation of EPC peak amplitude at low concentrations (< 1 mM), and 2) a decrease of peak amplitude and decay time constant with higher (> 1 mM) 2-PAM concentrations (Figure 11). The former effect could be due either to a presynaptic effect or to an alteration of postsynaptic processes such as an increase in the frequency of channel opening, as seen in patch clamp experiments. HI-6, on the other hand, produced a reduction in both peak amplitude and decay time constant at doses of 100 μM and above (Figure 12). There was a clear negative slope conductance seen in both plots at membrane potentials ranging from -100 to -150 mV at doses of 1 mM and above, suggesting the drug's ability to block the AChR-ionic channels in a voltage-dependent manner.

OP poisoning was achieved by perfusing the preparation for 1 hr with Ringer's solution containing 20 μM of OP and then with normal Ringer's solution for 1 hr to remove any excess of OP. This procedure resulted in a maximum inhibition of ChE as evidenced by a marked prolongation of EPC decay ($\geq$ 3 times that of control) with minimal direct effects of these compounds on the endplate. The prolongation of EPC decay by OP poisoning was seen even up to 4 hr after OP wash in control experiments. This allowed us to test the effect of oximes on such preparations (see Figures 13, 14 and 15). 2-PAM (100-500 μM) antagonized the effects on EPC parameters of soman (Figure 13) and VX, and HI-6 (100-500 μM) antagonized the effects of soman (Figure 14) and VX (Figure 15). Both 2-PAM and HI-6 (50 μM to 1 mM), at membrane potentials between -100 and + 50 mV, caused a voltage-independent reduction in τ_{EPC} in OP-poisoned muscle, which nearly reached control (pre-OP) levels. In addition, especially with HI-6 at hyperpolarized potentials, a steep, voltage-dependent decrease of τ_{EPC} was observed. Similar antagonism by both of the oximes against any of the four OPs studied was observed. However, this antagonistic effect of oximes diminished upon their removal from the bath (τ_{EPC} again increased to a level nearer to pre-oxime values), thus suggesting that the antagonism was merely a manifestation of the direct effects of oximes at the AChR-ionic channel complex rather than due to a reactivation of the phosphorylated AChE enzyme. This was supported by the biochemical studies in which 2-PAM up to 500 μM did not reactivate the VX-inhibited enzyme from frog sartorius muscle (Table 1). Qualitatively similar results were obtained when 2-PAM

was administered after the muscle was exposed to OPs for a brief period of 10 min.

Both these oximes accelerated the EPC decay in preparations pretreated with 10 μM of the reversible AChE inhibitor (-) physostigmine. Figure 16 illustrates such an interaction between (-) physostigmine and 2-PAM. (-) Physostigmine eliminated the voltage dependency of the EPCs decay time constant (Figure 14) which is the result of two opposing reactions namely AChE inhibition leading to slower EPC decay at all potentials and the channel blocking affect leading to acceleration of EPC decays at negative membrane potentials. Addition of 2-PAM caused further acceleration of EPC decay at all potentials indicating a direct channel blocking action for this oxime. Washing the preparation resulted in slower EPC decay but without loss of voltage sensitivity. This indicates that the AChR channel-blocking effect of the two drugs recovered earlier than the inhibition of the AChE enzyme by (-) physostigmine at the frog endplate region. Since the acceleration of EPC decay by these oximes is seen either in the presence of irreversible (OP) or reversible (physostigmine) ChE inhibitor, it is unlikely that such an effect is mediated through reactivation mechanisms.

Whereas in normal muscles the stochastic nature of channel-closing events determines the decay phase of the EPC, in muscles poisoned by an anticholinesterase (antiChE) inhibitor rebinding of ACh molecules occurs during the decay phase and results in a prolongation of the EPC. Under circumstances of ChE blockade, it is possible that a desensitizing agent could shorten the antiChE-prolonged decay by preventing receptor reactivation during the decay phase of the EPC. To ascertain whether the acceleration of EPC decay by 2-PAM and HI-6 in OP-treated muscles was a consequence of desensitization of AChR, we studied the effect of these oximes on the responses of denervated rat soleus muscle to micro-iontophoretically applied ACh. As shown in Figure 16, neither 2-PAM nor HI-6 affected the amplitude of the ACh pulses in a train, thus ruling out the involvement of a desensitization as a mechanism for oxime effects.

Patch clamp experiments with these oximes yielded some interesting observations. 2-PAM markedly increased the frequency of opening of ACh channels as observed in studies on the frog single muscle fibers (Figure 18). The significance of this effect is unclear; however, it may suggest the role of "activation" or "prevention of desensitization" of AChRs. This effect was not that marked in the case of HI-6. Both 2-PAM and HI-6 induced many brief interruptions during opening of the channels ("flickering"), which, at higher concentrations, resulted in bursts of short-lived open states (Figures 19 and 20). The mean channel open time was reduced to a great extent by both oximes, HI-6 being most potent for this effect (Figure 21). This channel-blocking effect of HI-6 correlates well with EPC results, in which this oxime produced a clear, voltage-dependent reduction of τ_{EPC}.

In summary, the voltage-dependent reduction of EPC decay time constant and peak amplitude by oximes (especially HI-6), the reversible antagonism of OP effect by both 2-PAM and HI-6, and a further acceleration of EPC

decay in the presence of physostigmine all indicate clearly the major involvement of a direct action of oximes at the ionic channels of the AChR. the reduction of both mean single-channel lifetime and conductance in the presence of 2-PAM and HI-6, seen in our patch clamp studies, confirms the above hypothesis. It may be concluded that the AChR channel-blocking effects of oximes may form one of the major mechanisms by which these drugs antagonize OP effects.

Correlation of the microphysiology of carbamate anticholinesterases and the endplate myopathy in rat soleus muscles.

It has recently been established that two different carbamates, physostigmine and neostigmine, have strikingly different microphysiological effects on nicotinic receptor/ion channel complexes. Physostigmine has a weak nicotinic-agonist effect and a strong channel-blocking effect, whereas neostigmine has a strong cholinergic-agonist effect and produces little channel block. In order to determine whether these differences can result in differing patterns of subjunctional myopathy at voluntary neuromuscular junctions, we used concentrations of the two drugs which produce identical levels of inhibition (50%) of whole-blood AChE activity. Furthermore, we applied the drugs to rat soleus <u>in vitro</u> neuromuscular preparations so that we could control the action potential frequency applied to the nerves.

A morphometric analysis of the subjunctional cytoplasmic area showed that stimulation at 5 Hz for 1 hr caused a 42% increase ($p < 0.001$). In contrast, exposure to neostigmine for 1 hr without stimulation caused a 253% increase over the control value. Subsequent stimulation at 5 Hz further expanded the endplate to 354% of the control value. Physostigmine exposure caused a significantly smaller (111%) increase and simultaneous 5 Hz stimulation caused a much smaller increment (to 132% of control value). We interpret the results according to the established hypothesis that endplate myopathy is driven by excess cholinergic agonism leading to excess ion accumulations. Our observations provide striking evidence that, at least under these controlled conditions. the expected differences between the ion fluxes, through nicotinic receptor/channel complexes induced by these two drugs, correlates with the degree of morphological damage subsequently observed at the endplates. The relative resistance of physostigmine-exposed junctions to further stimulation-induced damage is of particular significance.

The experiments also provided an opportunity to examine the presynaptic effects of these two antiChE agents by electron microscopy. Significant differences in this regard are also documented.

Protection by (+) physostigmine, the enantiomer of natural physostigmine, against lethality and myopathy induced by sarin.

Natural (-) physostigmine, has been shown to be effective as a pretreatment drug against the lethal effects of sarin (13). In addition, the soleus muscles of rats pretreated with (-) physostigmine (0.1 mg/kg, s.c.) for 30 min prior to injection of a sublethal dose of sarin (0.08

mg/kg, s.c.) showed an 86% reduction in the average dimensions of subjunctional lesions 1 hr after injection of sarin (15). Such results are usually interpreted to mean that transitory blockade by (-) physostigmine protects a critical portion of the enzyme from irreversible phosphorylation by the organophosphorus agent. When (-) physostigmine was injected s.c. (0.1 mg/kg) into rats, it blocked <10% of soleus muscle AChE.

Since (+) physostigmine was 200-fold less potent than (-) physostigmine in inhibiting junctional AChE of the soleus muscles (in vitro study), we used this compound to test the above hypothesis. Pretreatment of female Wistar rats (200-220 g) with 0.1, 0.3 and 0.5 mg/kg (+) physostigmine together with 0.5 mg/kg atropine (i.m.) 30 min prior to a 100% lethal dose of sarin (s.c.) reduced the lethality to 63, 29 and 23%, respectively. The electron micrographs in Figure 22 show (A) the myopathic changes in a soleus muscle 5 days after an injection with a sublethal dose of sarin (0.08 mg/kg). Figure 22 (B) and (C) shows the appearance of the muscles when the same dose of sarin was preceded by injection of 0.1 mg/kg (-) physostigmine and 0.3 mg/kg (+) physostigmine, respectively. There was a marked reduction in the severity and extent of myopathic damage induced by sarin in these rats (Table 2). The soleus muscles removed 1 hr after injection of 0.3 mg/kg (+) physostigmine in three rats showed virtually no inhibition of AChE. One hr after injection of a sublethal dose of sarin (0.08 mg/kg), the area covered by subjunctional lesions was 2018 $\pm$ 163 μm^2. Pretreatment of rats with (-) and (+) physostigmine before a lethal injection of sarin (0.13 mg/kg) reduced the subjunctional lesion size to 273 $\pm$ 15 and 289 $\pm$ 19 μm^2, respectively (Table 2). Moreover, examination of the muscles at day 5 after pretreatment with carbamates before sarin injection showed no detectable abnormality at the endplate region. A single injection of (-) physostigmine (0.1 mg/kg) alone produced minor but detectable damage of the subjunctional region, which was interpreted to result from AChE inhibition. Therefore, we examined the effects of (+) physostigmine injected alone in rats at doses of 0.1, 0.3 and 0.5 mg/kg. The degree of myopathy produced by (+) physostigmine was significantly lower in comparison to (-) physostigmine. This is consistent with the weak AChE-inhibitory activity of (+) physostigmine.

In conclusion, the prophylactic effectiveness of (+) physostigmine against the toxic effects of sarin suggests that mechanisms other than AChE blockade may underlie the protection afforded by carbamates in organophosphorus poisoning. This protection is most likely due to the ability of (+) physostigmine and (-) physostigmine to block the postsynaptic AChR.

Optical isomers as powerful tools to unveil the mechanism by which physostigmine and mecamylamine protect against organophosphate poisoning.

a) Effects of the (+) and (-) stereoisomers of physostigmine on endplate currents and single-channel currents.

The (+) stereoisomer of physostigmine offered protection against OP compounds similar to that provided by the natural (-) isomer. Since (+) physostigmine is a very weak antiChE agent, the protection afforded by this agent must not be related to the AChE carbamylation-reactivation process.

To determine the molecular mechanism(s) responsible for the protection afforded by (+) physostigmine, a study was done, using voltage- and patch-clamping techniques. (-) physostigmine, at low concentrations (0.2-2.0 μM), increased the peak amplitude and prolonged the time constant of decay of EPCs recorded from frog sartorius muscles (16), effects that are mostly due to the drug's antiChE activity. (+) Physostigmine did not produce these antiChE type effects on the EPCs, but at concentrations > 20 μM produced blocking effects (Figure 23). Both stereoisomers blocked the EPCs by decreasing the peak amplitude and shortening the τ_{EPC} in a concentration- and voltage-dependent manner (ref. 16 and Figure 23). τ_{EPC} was decreased with increasing drug concentrations, and the voltage sensitivity of τ_{EPC} was gradually reduced as the concentration of the blocking agent was increased. Whereas double exponential decays were produced by high concentrations of (-) physostigmine, at depolarized potentials, the decay remained single exponencial functions of time at all concentrations of (+) physostigmine tested. These data suggest that although not having antiChE activity like (-) physostigmine, (+) physostigmine is also a blocker of the open conformation of the AChR.

At the single-channel current level, using the patch-clamp technique, (+) physostigmine, like the natural (-) isomer, acted as an agonist of the AChR. (-) physostigmine induced currents with many very fast flickers (16) while (+) physostigmine-activated currents were well separated pulses without flickers, like those activated by ACh (Figure 24). Both isomers also blocked their own channels (see ref. 16 and Figures 24 and 25). Although both isomers acted as agonists, (+) physostigmine activated channels at concentrations higher than 10 μM, whereas the natural (-) isomer activated channels at concentrations higher than 1 μM. When in the presence of ACh, each stereoisomer acted as an open channel blocker, producing a concentration-dependent decrease in the channel open time (ref. 16 and Figure 25). (+) physostigmine, on ACh-activated channels, did not produce discernible bursting activity, while (-) physostigmine induced bursts with many flickers. Therefore, the protection afforded by physostigmine against irreversible ChE blockers may reside in its ability to block the postsynaptic AChR directly in the early phases of OP poisoning.

b) Effects of (+) and (-) optical isomers of mecamylamine on endplate currents and on single-channel currents activated by acetylcholine.

Mecamylamine is well known for its actions as a competitive antagonist of the nicotinic AChR at the autonomic ganglia. As a nonquaternary ammonium compound it would be expected to gain access readily to the central nervous system. It has also been shown to be a very powerful noncompetitive blocker of the nicotinic neuromuscular AChR (17). Owing to these characteristics, mecamylamine was combined with physostigmine in the pretreatment regimen against OP poisoning, and the effectiveness of the pretreatment was found to be greatly enhanced (18). A study of the optical isomers was done in order to determine the precise mechanism(s) responsible for its effectiveness and whether or not the isomers have different effects on the AChR. A voltage- and time-dependent depression of peak EPC amplitude was produced by the (+) and (-) isomers (Figures 26 and 27).

These effects were more significant with (+) mecamylamine as revealed by a marked hysteresis loop observed in the current-voltage relationship over the entire range of hyperpolarized potentials. The hysteresis loop indicated a blockade of the AChR in closed conformation. Both isomers reduced τ_{EPC} and removed the voltage dependence of this parameter, in accordance with an open channel blocking mechanism. (+) Mecamylamine was more potent than (-) mecamylamine in depressing τ_{EPC}, with IC_{50} of 8 μM and 16 μM for (+) and (-) mecamylamine, respectively. At the single-channel current level, both isomers decreased the mean channel open time, an effect predicted for open channel blockers. Nevertheless, (+) mecamylamine was more effective in decreasing the channel lifetime than the (-) stereoisomer. Both isomers produced channels well separated events, i.e. no bursting activity was observed. (+) mecamylamine, as a powerful desensitizing agent, was potent in decreasing the frequency of channel openings, indicating that (+) mecamylamine should be the most effective against cholinergic hyperactivation following OP poisoning. Studies such as these are important not only for explaining the mechanism(s) of action of agents that have already been shown to be effective in protecting against OP challenge, but also, in view of the detailed information gained, in providing the guidelines for an accurate prediction of effectiveness of putative new prophylactic agents.

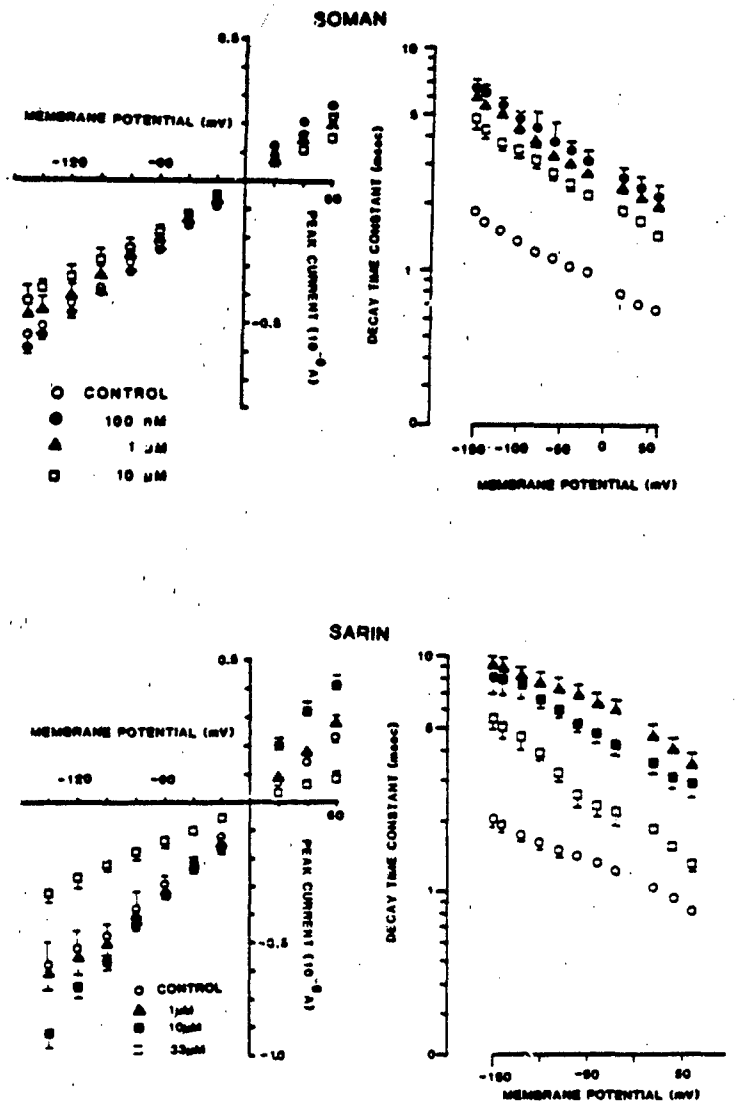

Figure 1. Effects of soman and sarin on EPCs recorded from frog sciatic nerve-sartorius muscle preparation.

Both compounds at low concentrations increased EPC peak amplitude and decay time constant, while at higher doses they decreased these parameters. The former effect is due to AChE inhibition, whereas the latter is indicative of a direct action on the AChR.

Note that soman is more potent than sarin in producing the blocking action.

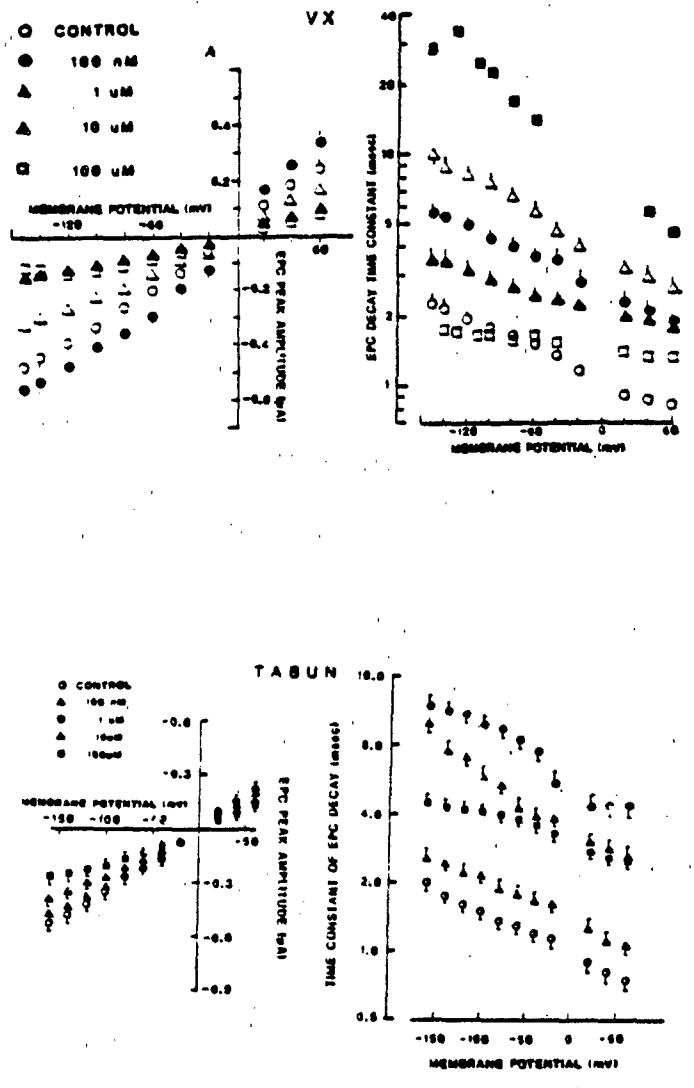

Figure 2. Effects of VX and tabun on EPCs recorded from frog sciatic nerve-sartorius muscle preparations.

Both compounds at low concentrations increased τ_{EPC}, while higher doses decreased it. A facilitation followed by depression of EPC peak amplitude was induced by VX in a dose-dependent fashion, whereas only depression was observed with tabun at all concentrations used.

Note the marked voltage-dependent effect of VX on both EPC parameters. There was a double exponential decay of EPC at 100 μM VX, the faster phase represented by open squares and the slower phase by filled squares in the decay plot.

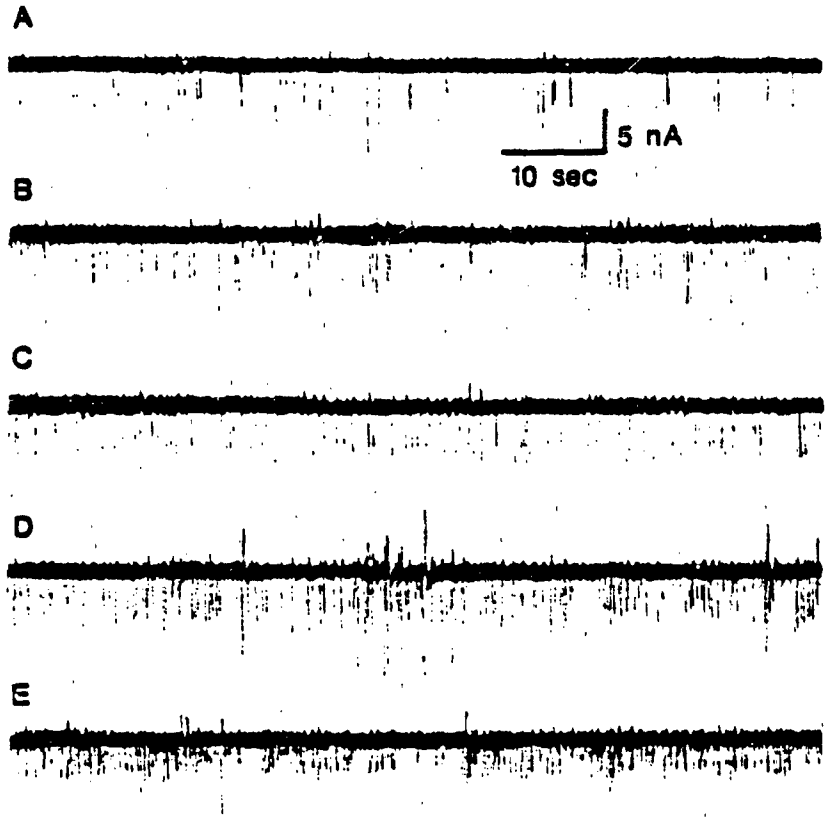

Figure 3. Effect of VX on the frequency of spontaneously occurring MEPCs recorded from frog sartorius muscle.

Tracings A-E are MEPCs obtained from a single cell from a frog sartorius muscle pretreated with diisopropylfluorophosphate (DFP) (1 mM; 30 min) and held at -80 mV membrane potential. Following exposure to DFP, the muscle was washed for 60 min before records were obtained in the absence (A) and in the presence of 1 (B), 5 (C), 10 (D) or 50 (E) μM VX.

None of the other three OPs significantly affected MEPC frequency.

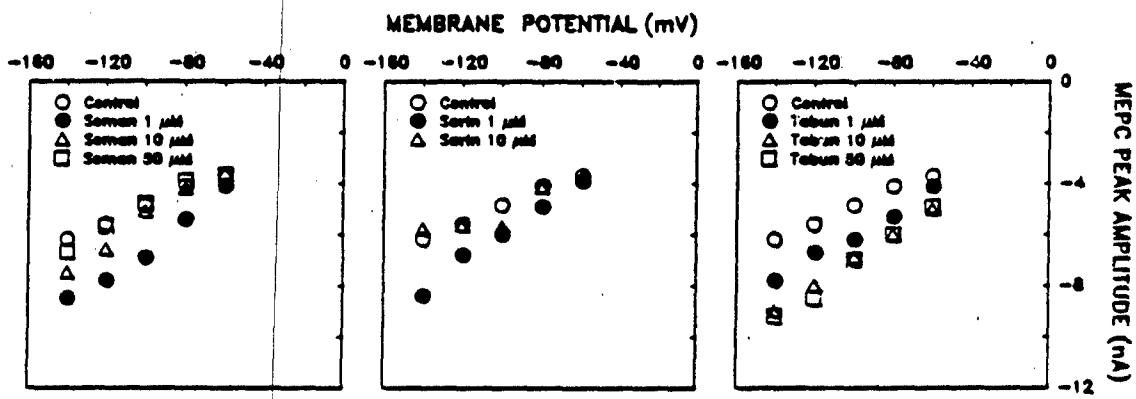

Figure 4. Effect of soman, sarin and tabun on MEPC peak amplitude recorded from frog sartorius muscle in the presence of 3×10^{-7} M tetrodotoxin.

Soman and sarin increased the peak amplitude at low concentration (1 μM) but decreased the amplitude towards control values at concentrations of ≥ 10 μM. On the other hand, tabun caused only a facilitatory effect.

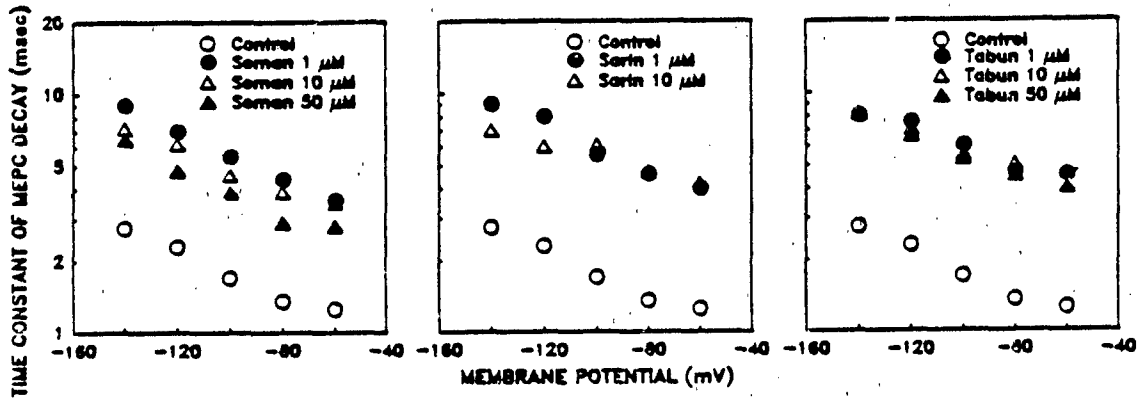

Figure 5. Effect of soman, sarin and tabun on MEPC decay time constant recorded from frog sartorius muscle in the presence of 3×10^{-7} M tetrodotoxin.

All the three OPs produced maximal increase in τ_{EPC} at 1 μM. Higher concentrations ($\geq$ 10 μM) reduced the τ_{EPC} from the already enhanced values, which was seen clearly in the case of soman and sarin.

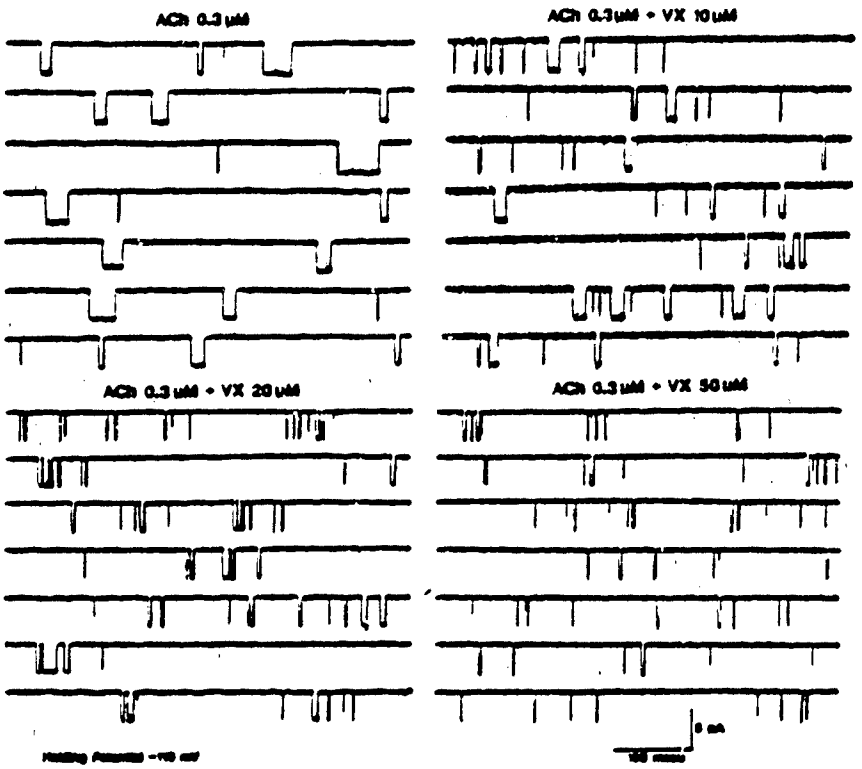

Figure 6. Samples of ACh-activated channel currents, recorded from frog interosseal muscle, in the presence of various concentrations of VX.

Records were obtained from isolated frog muscle fibers, using cell-attached patch configurations. Temperature 10°C. Filter band width: 3 kHz. Holding potential, -110 mV. Note the dose-dependent blockade of channel open time.

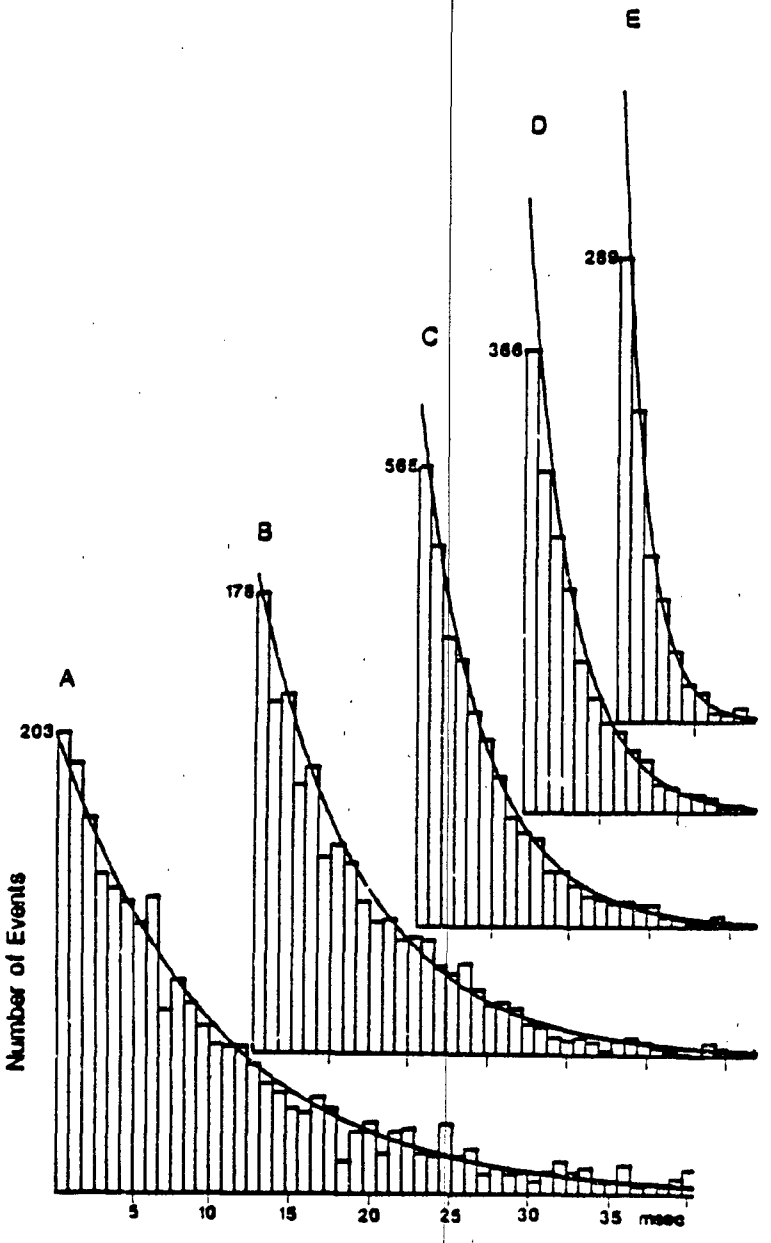

Figure 7. Open time histograms of channel currents, recorded from frog intraosseal muscle, activated by ACh in the presence of VX.

Single-channel currents were recorded, using cell-attached patch configuration with a pipette containing ACh (0.3 μM) either alone (A) or together with 5 (B), 10 (C), 20 (D) or 50 (E) μM VX. Mean channel open times as determined by linear regression on the logarithms of the bin amplitude were 9.7 (A), 6.5 (B), 4.11 (C), 2.8 (D) and 1.5 (E) msec. Potential was held between -120 and -130 mV.

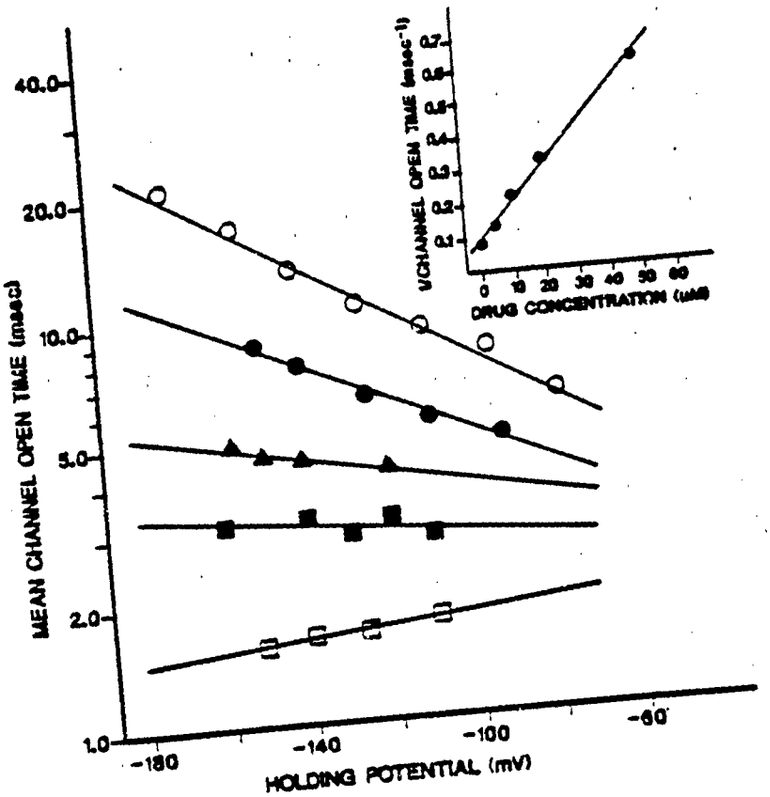

Figure 8. Voltage- and concentration-dependent effects of VX on the channel open times, recorded from frog interosseal muscle.

Relationship between the logarithm of the mean channel open times and holding potentials from single channel recordings obtained with ACh (0.3 μM) either alone (○) or together with 5 (●), 10 (▲), 20 (■) or 50 (□) μM VX.

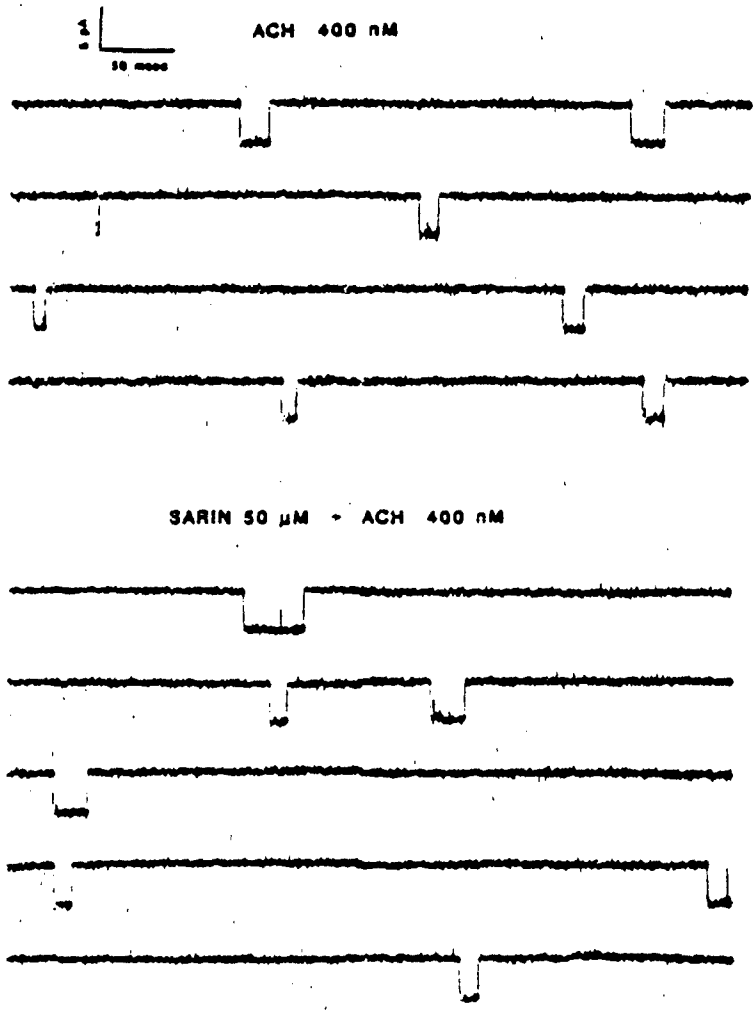

Figure 9. Samples of ACh-activated channel currents, recorded from frog interosseal muscle, in the absence and presence of sarin.

Methods similar to those for VX. Holding potential, -165 mV. Note that unlike VX, this compound did not significantly change the mean channel open time up to a concentration of 50 µM.

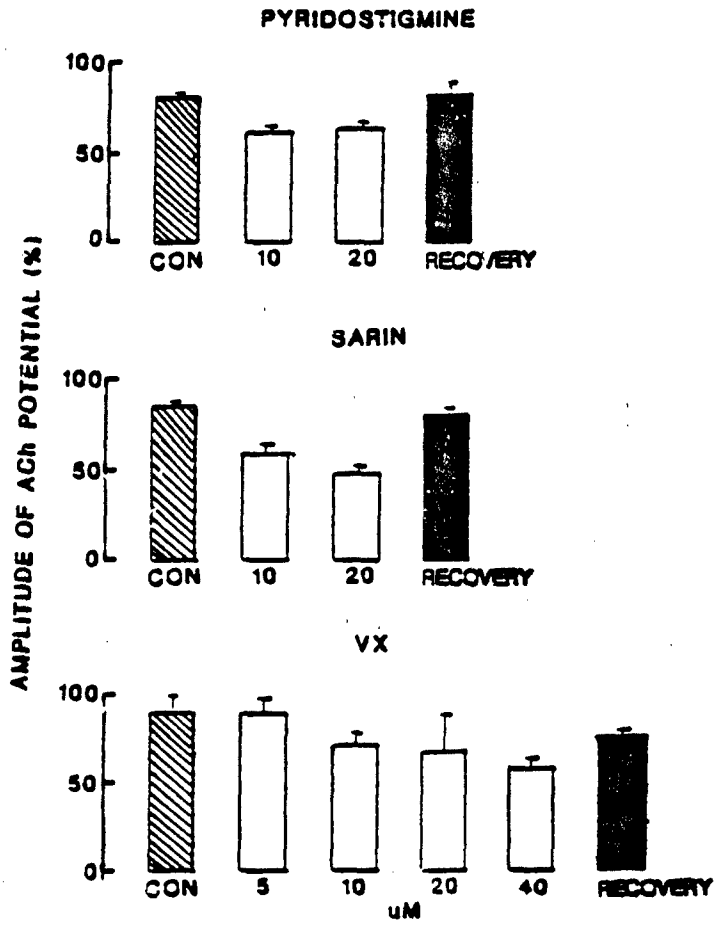

Figure 10. Effect of pyridostigmine, sarin and VX on desensitization in the soleus muscle.

Amplitudes of 1st and every 10th response in a train of 100 responses were measured and expressed as percent amplitude of 1st ACh potential in a train. For the purpose of this figure responses elicited by the 90th and 100th ACh pulse were pooled and expressed as percent of 1st response. In control (CON) conditions, there is only a 10-15% decrement in ACh response, whereas in the presence of pyridostigmine or OP agents there is a 30-50% decrement in responses due to desensitization. Vertical bars indicate SEM of values obtained in at least 3 trials for each concentrations.

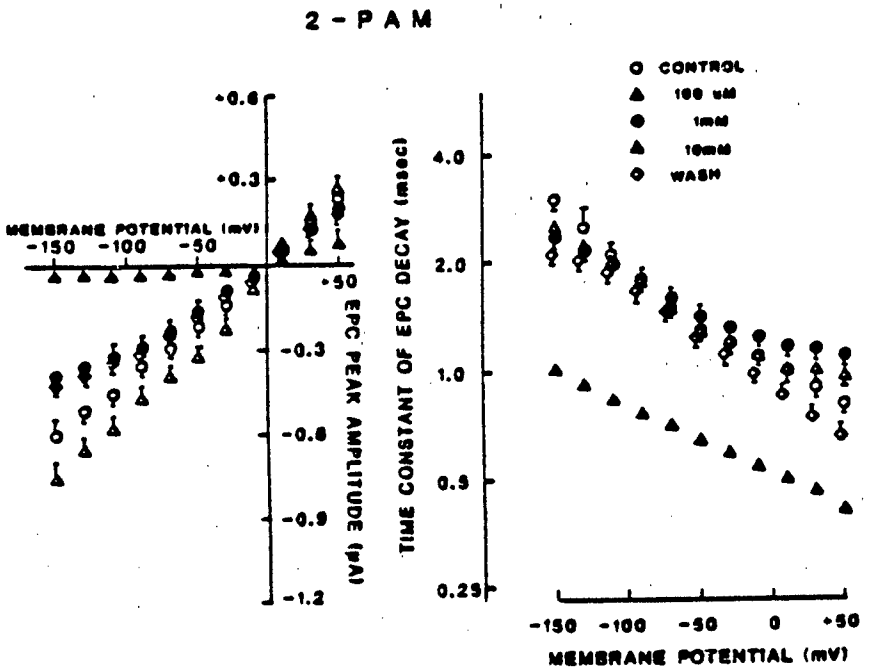

Figure 11. Effects of 2-PAM on EPC peak amplitude and time constant of EPC decay (τ_{EPC}), recorded from frog sartorius muscle.

2-PAM (100 μM) increased EPC peak amplitude, whereas doses of 1 mM and above depressed it.

Note the slight depression of τ_{EPC} by 2-PAM at very negative holding potentials.

H I - 6

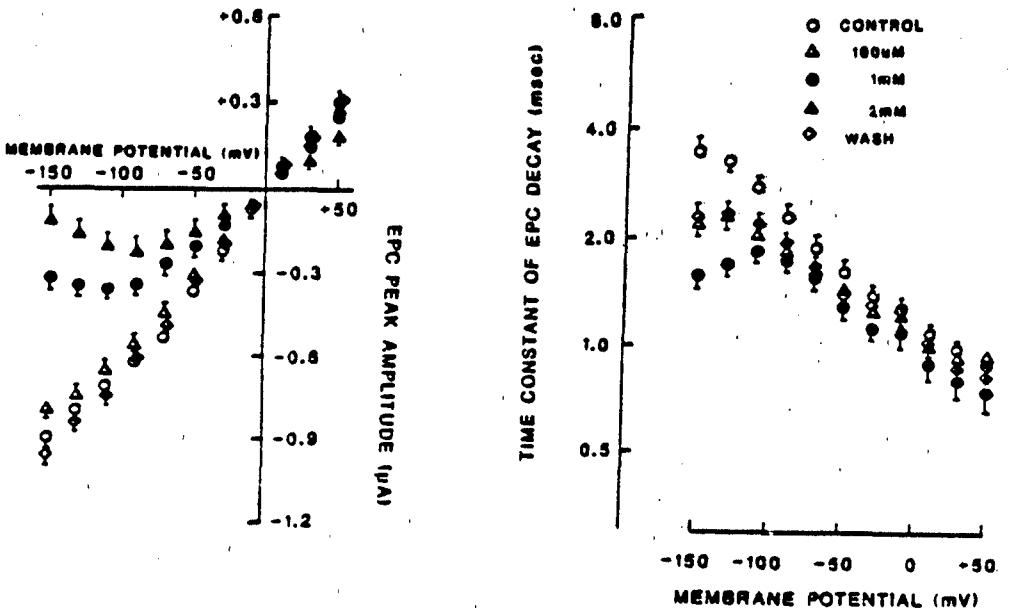

Figure 12. Effects of HI-6 on EPC peak amplitude and τ_{EPC}, recorded from frog sartorius muscle.

HI-6 (100 μM) produced a voltage-dependent depression of both parameters.

Note the slope reversal in both plots at negative membrane potentials ranging from -100 mV.

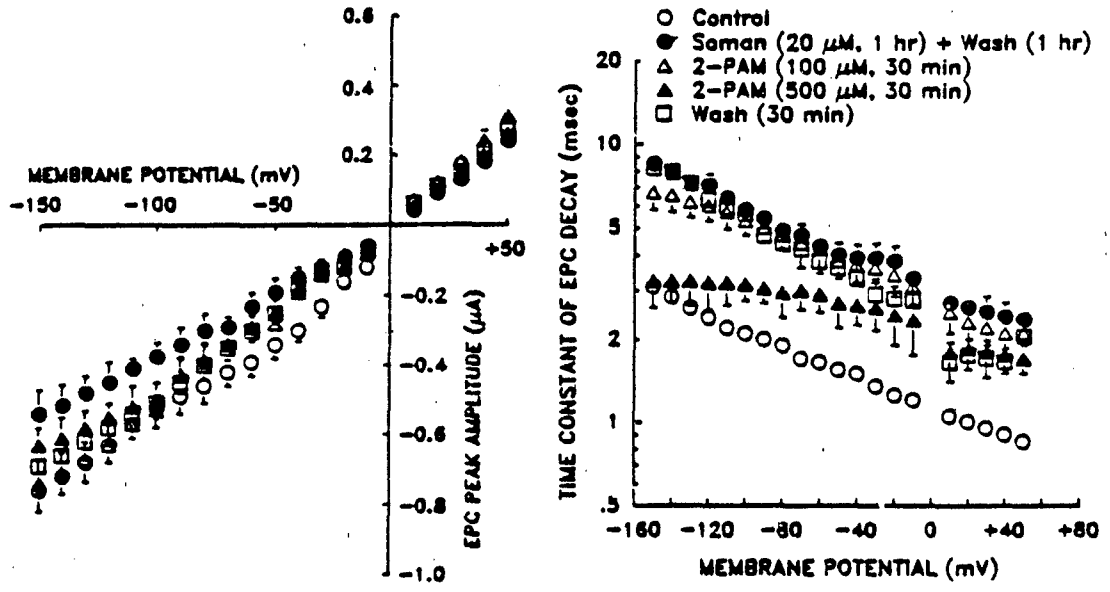

Figure 13. Soman-2-PAM interaction as exhibited by their effects on EPC parameters recorded from frog sartorius muscle.

Treatment of the muscle with soman (or any OP) for 1 hr and a subsequent wash with normal Ringer's solution for 1 hr resulted in a marked enhancement of τ_{EPC} and a slight decrease in EPC peak amplitude. Further treatment with 2-PAM caused a reversal of the OP effect towards control values on both parameters.

Note the voltage-dependent reduction of τ_{EPC} by 2-PAM in the OP-treated muscle, which is more evident when compared to that observed in a preparation untreated with an OP.

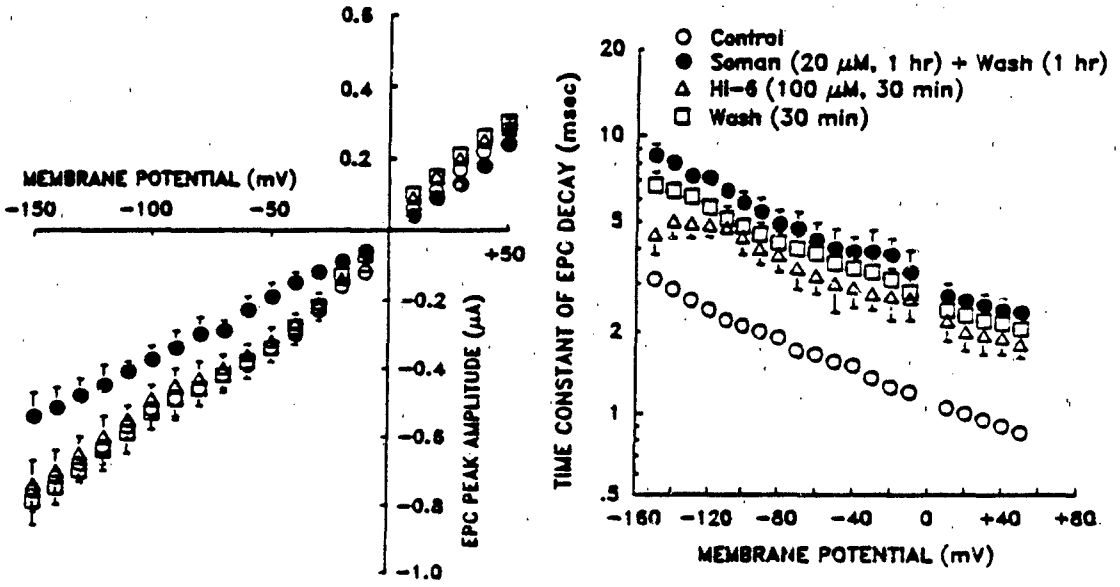

Figure 14. Soman-HI-6 interaction as exhibited by their effects on EPC parameters recorded from frog sartorius muscle.

Treatment of the muscle with soman (or any OP) for 1 hr and a subsequent wash with normal Ringer's solution for 1 hr resulted in a marked enhancement of τ_{EPC} and a slight decrease in EPC peak amplitude. Further treatment with HI-6 caused a reversal of the OP effect towards control values on both parameters.

Note the voltage-dependent reduction of τ_{EPC} by HI-6 in the OP-treated muscle, which is more evident when compared to that observed in a preparation untreated with an OP.

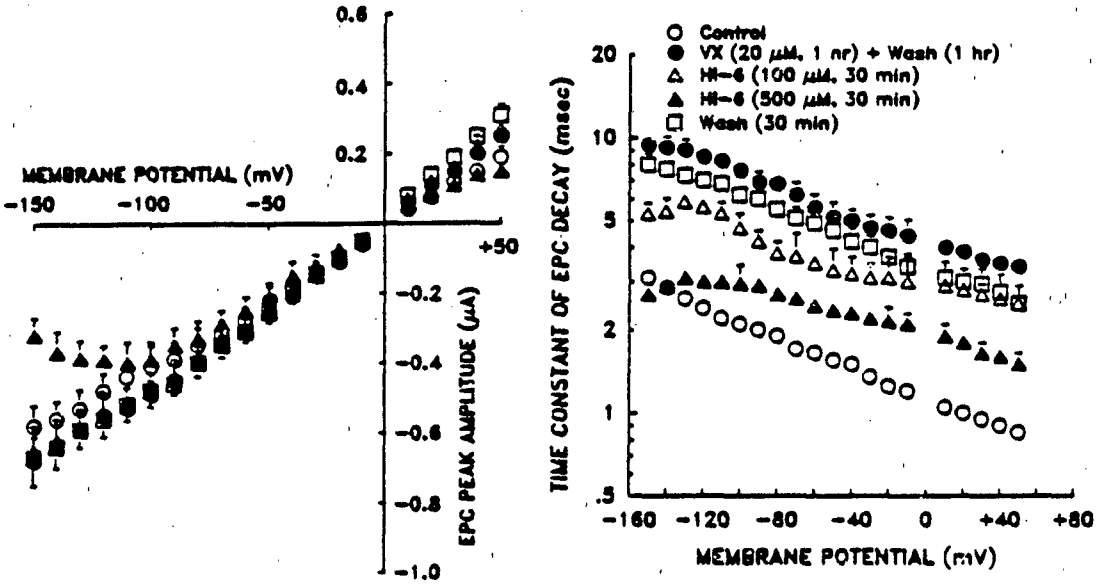

Figure 15. VX-HI-6 interaction as exhibited by their effects on EPC parameters recorded from frog sartorius muscle.

HI-6 also produced a reversal of the effects of VX (and other OPs) on EPC.

Question: Is the reversal of OP effect on EPC by oximes HI-6 and 2-PAM due solely to reactivation of phosphorylated AChE?

ANSWER: No.

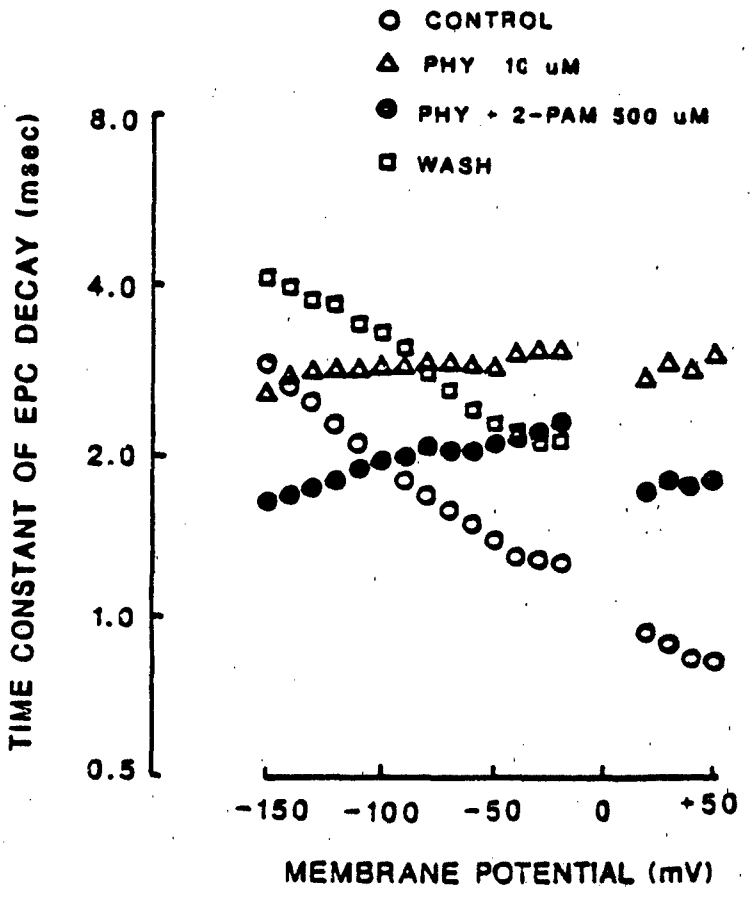

Figure 16. Interaction of 2-PAM with reversible AChE inhibitor on τ_{EPC} recorded from frog sartorius muscle.

2-PAM (and also HI-6) produced a clear depression of τ_{EPC} in muscle preparations treated with the reversible ChE inhibitor physostigmine. This effect also indicates the direct effect of oximes at the AChR-complex.

The blockade of τ_{EPC} seen in the presence of 2-PAM and HI-6 either alone or in the presence of ChE inhibitors is due to their channel-blocking effects, as seen in single-channel studies (see Figures 19 and 20).

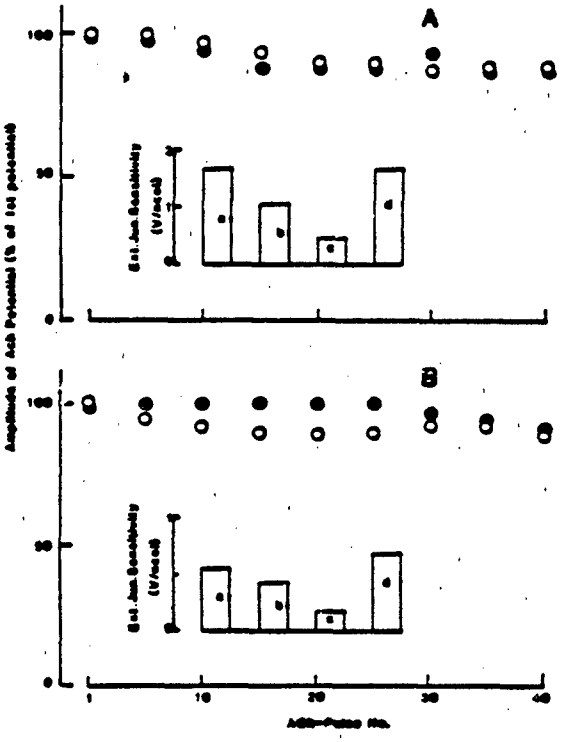

Figure 17. Sensitivity of the extrajunctional region of the chronically denervated soleus muscle of the rat to microiontophoretically applied ACh in the presence of 2-PAM (A) and HI-6 (B).

About 40 ACh pulses of 0.5 msec duration were applied to the extrajunctional region at 1 Hz and the resultant potentials were recorded intracellularly. The amplitudes of subsequently evoked ACh potentials in the train are plotted as percentages of the potential elicited by the first ACh pulse in the train. (○) Control; (●) in the presence of 2-PAM and HI-6. Note that the values obtained in the presence of drugs are not significantly different from those of control. The insets in A and B are the histograms showing the extrajunctional sensitivity (V/nC) to iontophoretically applied ACh in the absence and in the presence of drugs and after 60 min wash. The bars marked a-d in A are control, 2 mM 2-PAM, 4 mM 2-PAM, and 50 min after wash, respectively. The bars a-d in B are control, 0.5 mM HI-6, 1 mM HI-6 and 60 min after wash, respectively.

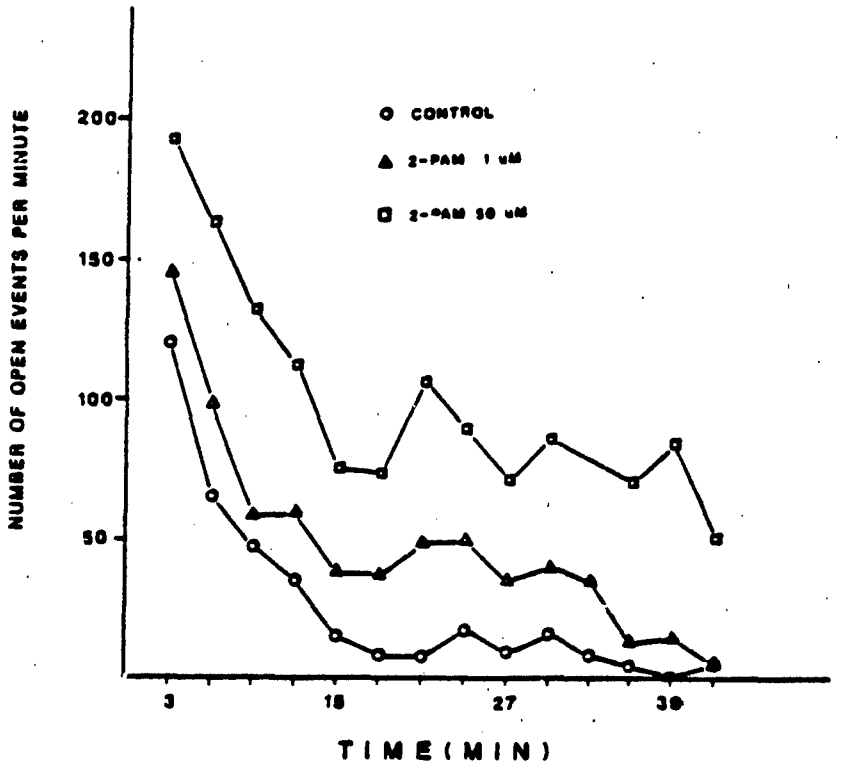

Figure 18. Frequency of channel opening activated by ACh in the absence and in the presence of 2-PAM, recorded from frog interosseal muscle.

Single-channel currents were recorded under cell-attached patch configuration. Each channel opening was counted as a single event only when it was separated from the previous closure by at least 8 msec. Pipette potential was held at -100 mV. Each line represents the mean number from at least three separate fibers on which successful recordings could be done for a period of at least 40 min.

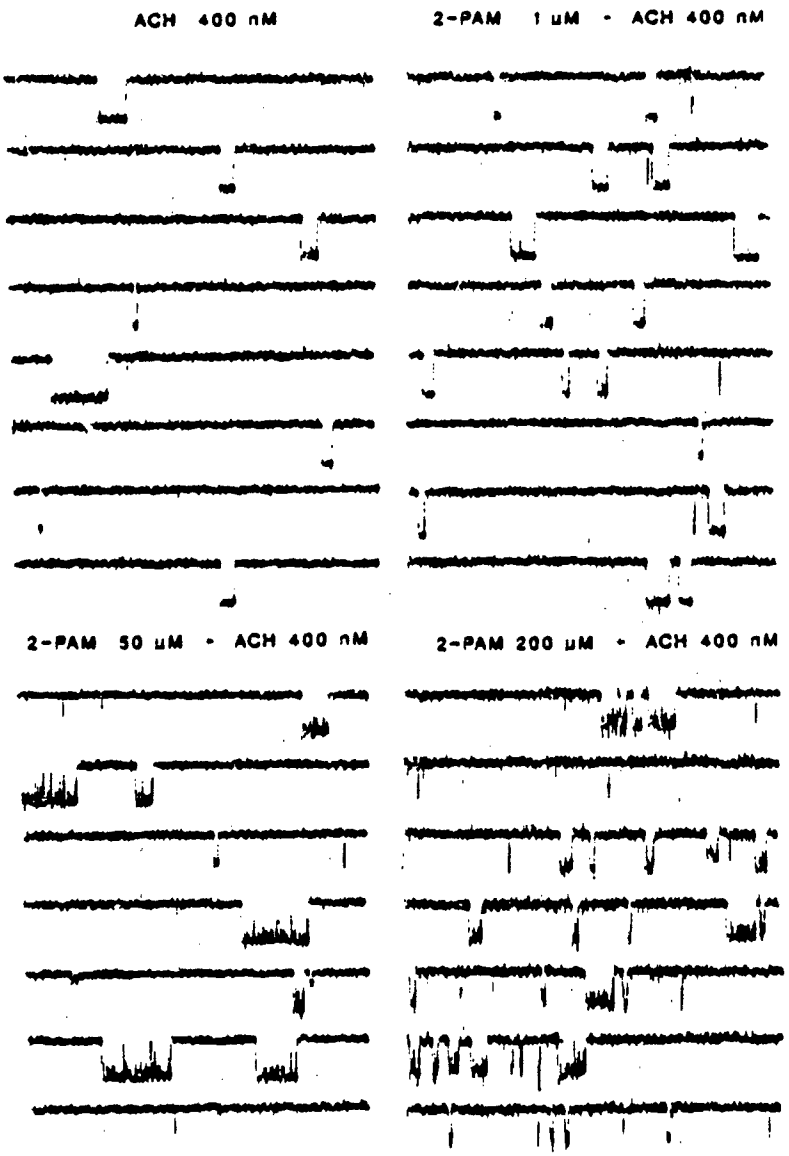

Figure 19. Samples of ACh-activated channel currents, recorded from frog interosseal muscle in the presence of various concentrations of 2-PAM.

Single-channel currents were recorded from frog muscle fibers under cell-attached patch configuration with a pipette containing ACh either alone or together with different concentrations of 2-PAM. Potential was held at -140 mV.

Note the graded increase in the flickering of the channels and the subsequent blockade of the channel open time. Also, there is an increase in the frequency of channel opening in the presence of 2-PAM.

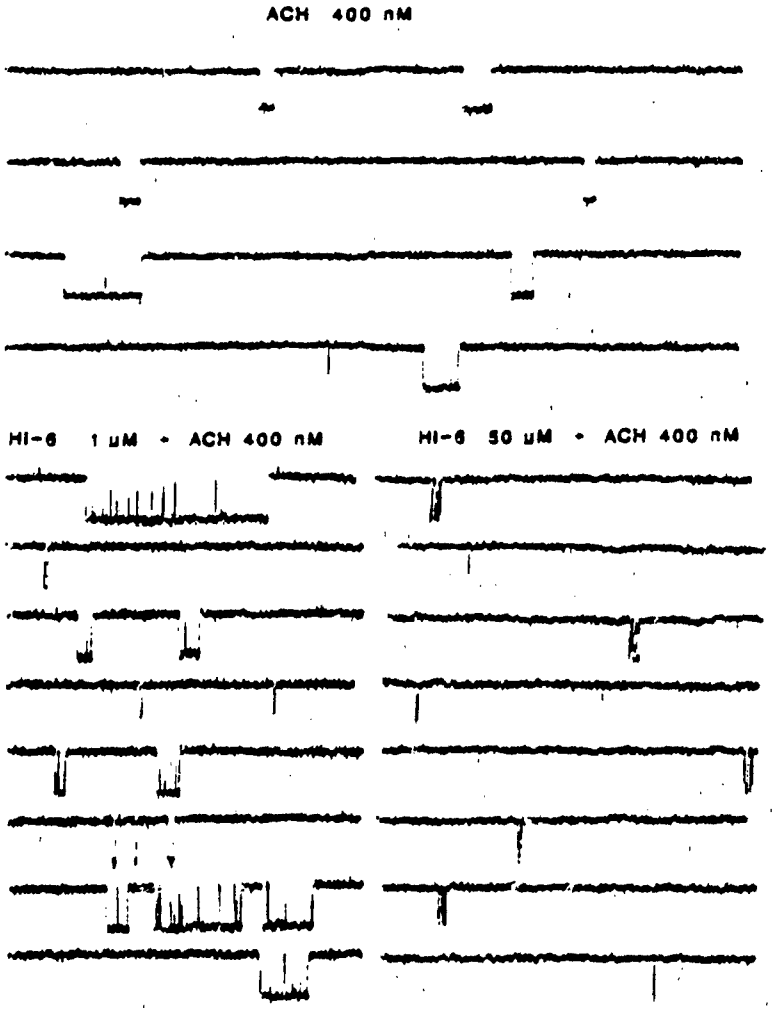

Figure 20. Samples of ACh-activated channel currents, recorded from frog interosseal muscle in the presence of various concentrations of HI-6.

Potential was held between -130 and -140 mV.

Note the drastic reduction in open time in the presence of HI-6.

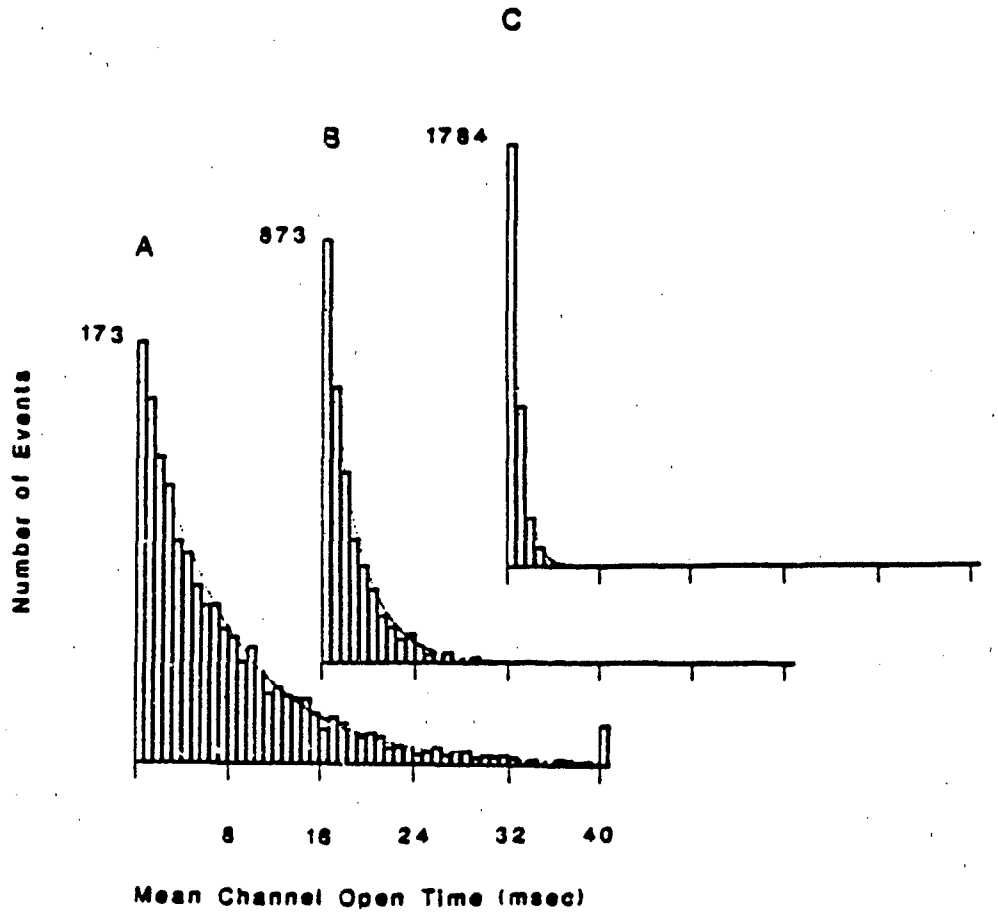

Figure 21. Open-time histograms of channels activated by ACh in the presence of 2-PAM and HI-6, recorded from frog interosseal muscle.

A Control ACh, 400 nM; mean from seven separate patches; mean open time = 8.20 msec; total number of events = 2112.

B 2-PAM 50 μM + ACh 400 nM; mean from two patches; mean open time = 2.72 msec; total number of events = 2897.

C HI-6 50 μM + ACh 400 nM; mean from two patches; mean open time = 0.87 msec; total number of events = 2802.

Potential was held between -130 and -140 mV.

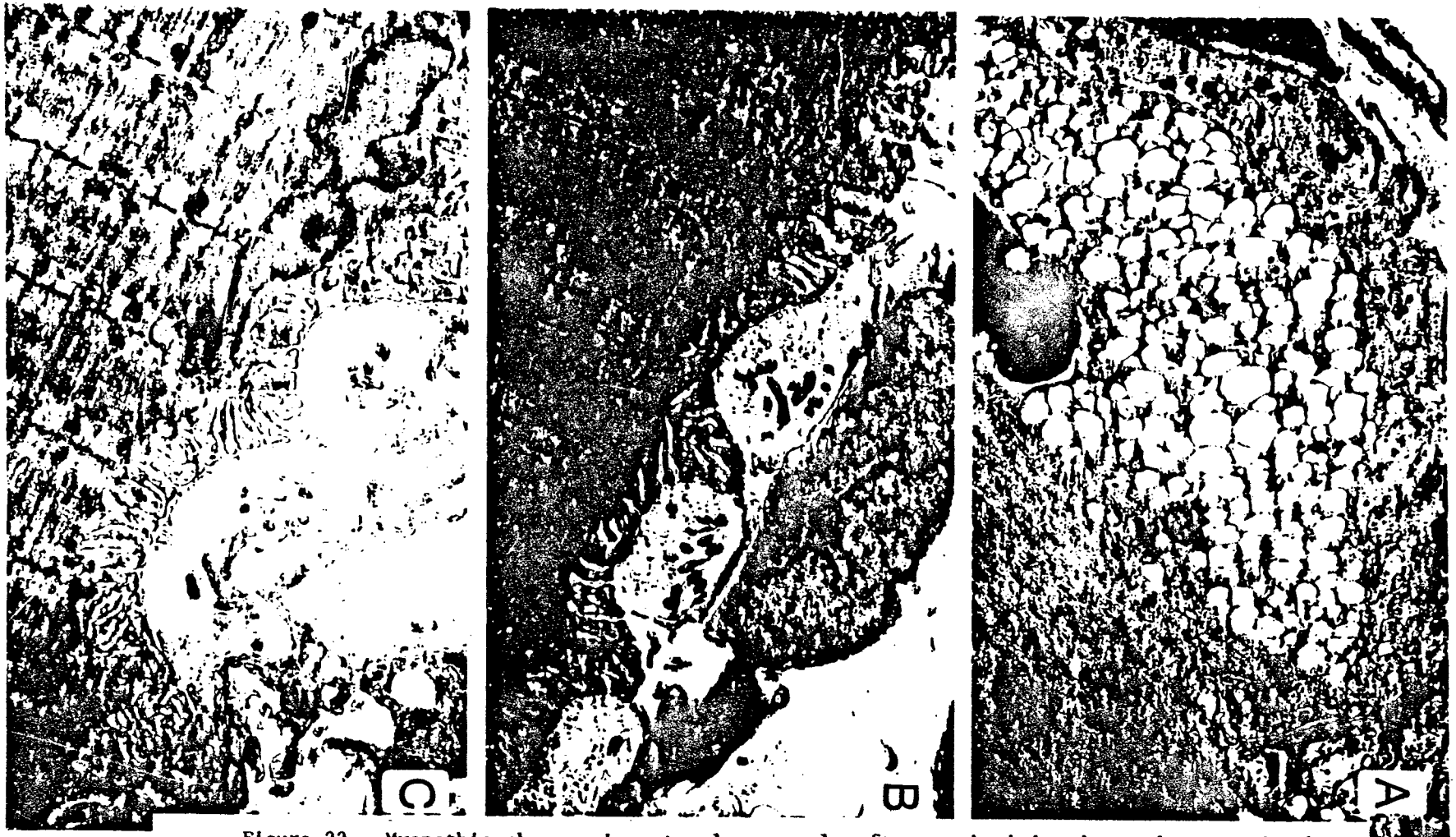

Figure 22. Myopathic changes in rat soleus muscle after sarin injection and protection by (-) and (+) physostigmine.

Electron micrographs of motor endplates of soleus muscles of the rat. Female Wistar rats (200-220 g) were injected s.c. with sarin (80 μg/ml). (A) Five days after a single sarin injection; (B) and (C) 5 days following sarin injection as in (A) except that 100 μg/kg (-) physostigmine and 300 μg/kg (+) physostigmine, respectively, were injected 30 min prior to

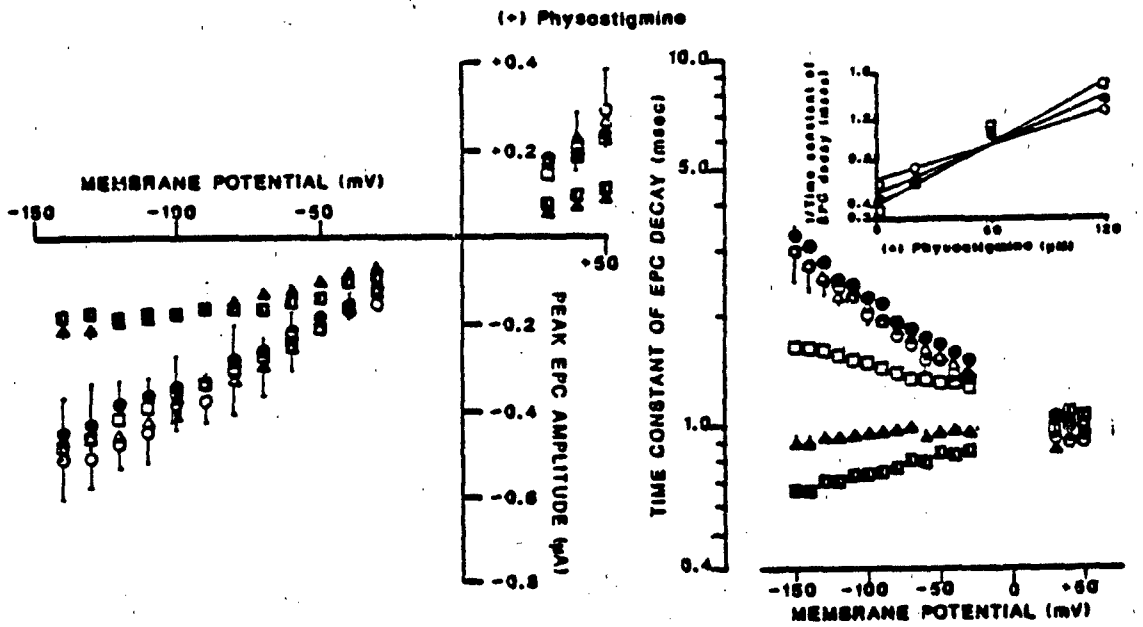

Figure 23. Concentration- and voltage-dependent effects of (+) physostigmine on the current amplitude and the decay time constant of the EPCs recorded from frog sartorius muscle.

Left: I-V relationship in the absence (○) and in the presence of (+) physostigmine 0.2 (●), 2.0 (△), 20.0 (□), 60.0 (▲) and 120.0 μM (■). Each symbol represents the mean obtained from at least six fibers observed in five or more muscles. Errors shown are S.E.M. Right: Relationship between time constant of EPC decay and holding potential. Inset: Relationship between the reciprocal of the time constant of EPC decay and drug concentration. Membrane potentials: -60 (○), -100 (●) and -140 (□) mV. Solid lines represent the best fit obtained by linear regression.

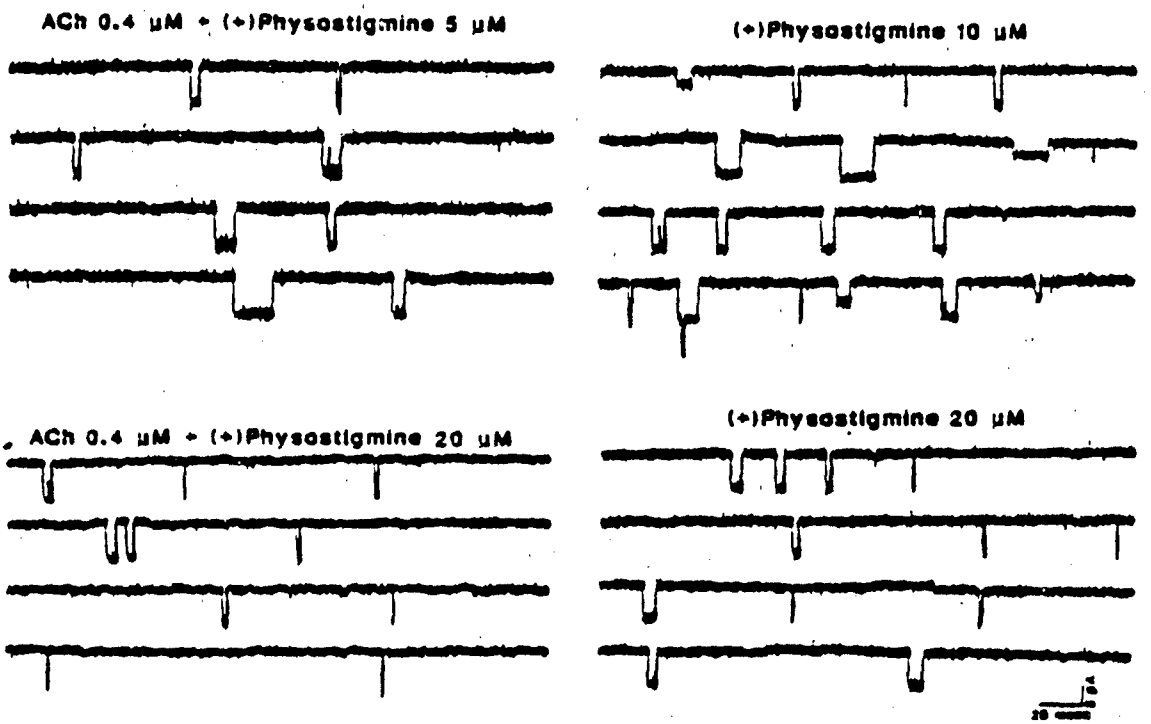

Figure 24. Samples of single-channel currents, recorded from frog interosseal muscle, activated by 10 μM and 20 μM (+) physostigmine alone in the patch pipette and by ACh in the presence of 5 μM and 20 μM (+) physostigmine.

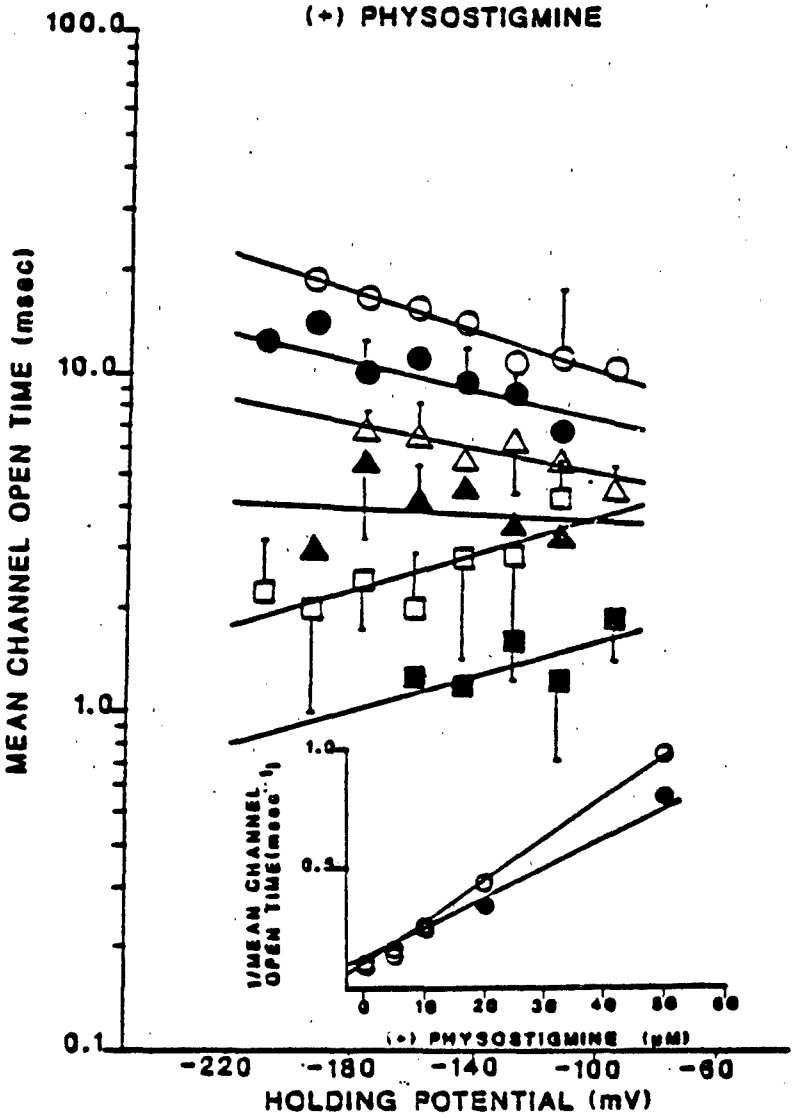

Figure 25. Effects of (+) physostigmine on the open times of ACh-activated single-channel currents recorded from frog interosseal muscle.

Voltage dependence of mean channel open times under control conditions (ACh alone, ○) and in the presence of 1 (●), 5 (△), 10 (▲), 20 (□) and 50 (■) μM (+) physostigmine. Inset: Relationship between the reciprocal of mean channel open time and drug concentration. Membrane potentials: -140 (○) and -180 (●) mV. Solid lines represent the best fit obtained by linear regression. Some points were pooled together at 20-mV intervals of the holding potential. Each symbol represents the mean with its standard deviation.

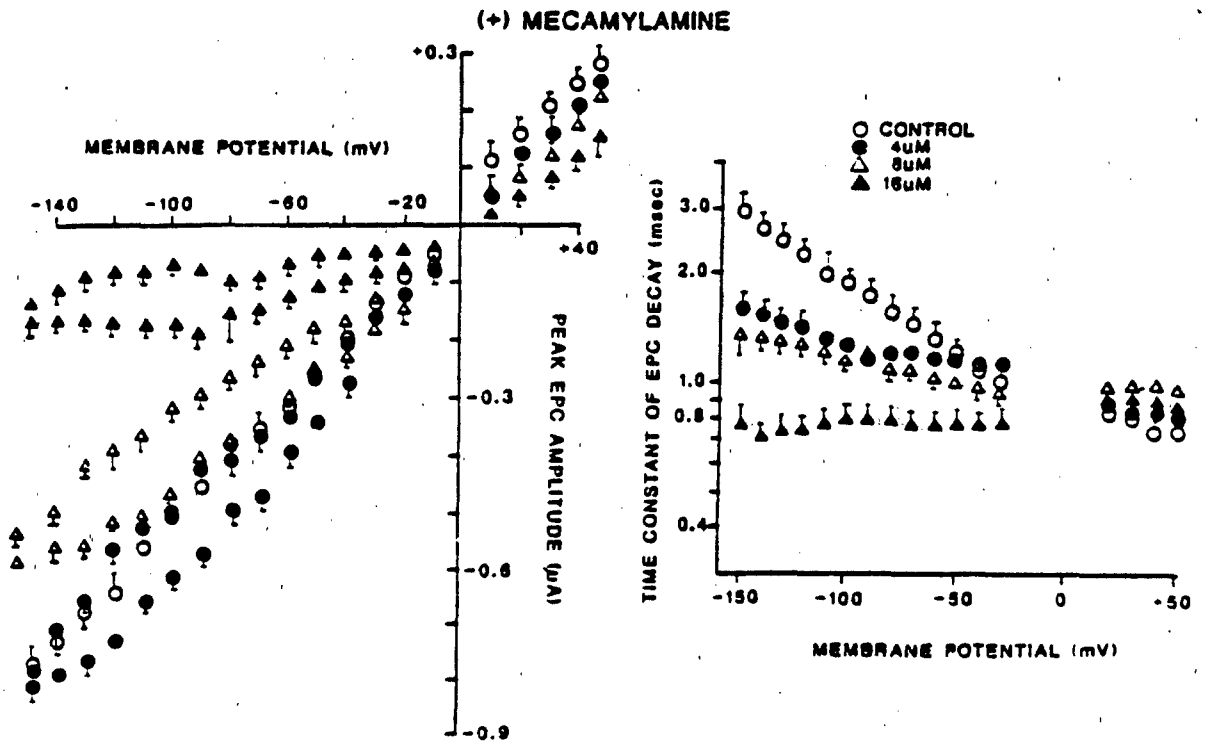

Figure 26. Concentration- and voltage-dependence of peak amplitude (left) and decay time constant (right) of EPCs recorded from frog sartorius muscle in the presence of high concentrations of (+) mecamylamine.

(○) control, (●) 4, (△) 8, and (▲) 16 μM (+) mecamylamine. A time-and voltage-dependent depression of the EPC peak amplitude is evident at hyperpolarized potentials. This effect was practically abolished when the duration of the conditioning pulse was shortened from 3 sec to 20 msec. The hysteresis seen with 3-sec conditioning pulses suggests some degree of desensitization of the nicotinic AChRs. (+) Mecamylamine also decreased the decay time constant of decay and induced an apparent loss of the voltage-dependence seen under control conditions, suggesting a blockade of the ion channel in its open conformation.

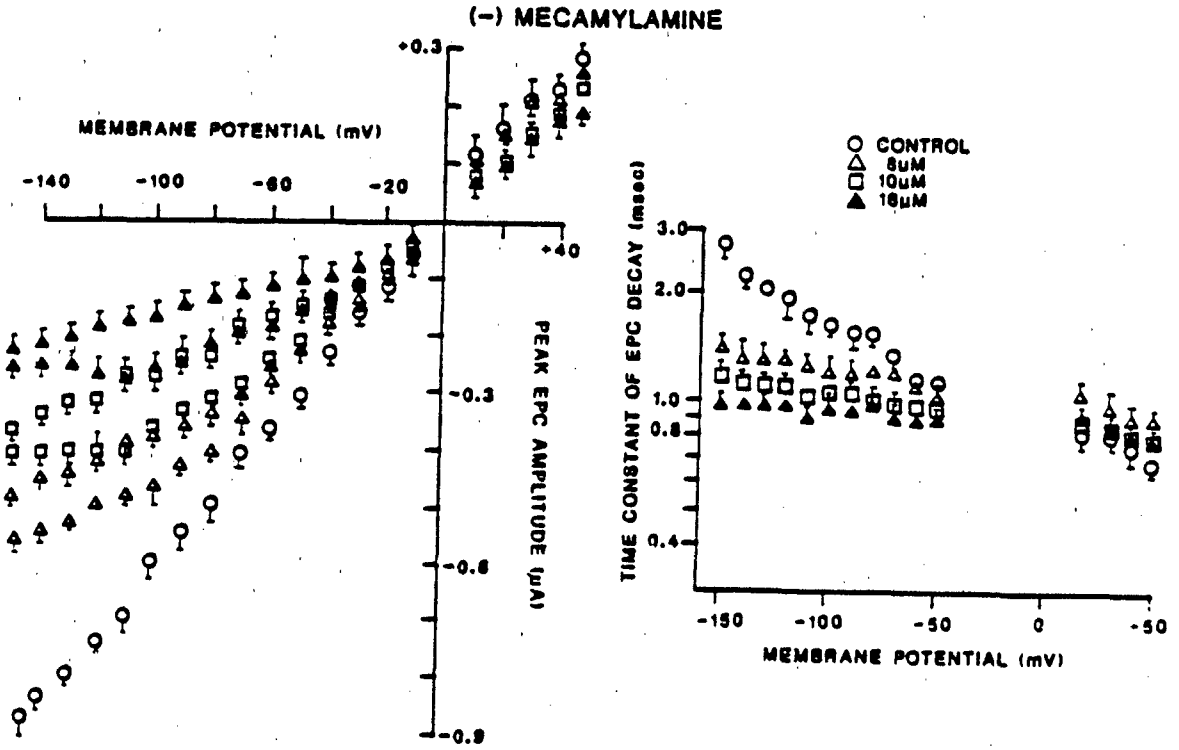

Figure 27. Concentration- and voltage-dependent effects of (-) mecamylamine on EPCs recorded from frog sartorius muscle.

Peak amplitude (left) and decay time constant (right) of EPCs in control conditions (○) and in the presence of high concentrations of (-) mecamylamine: (△) 8, (□) 10, and (▲) 16 μM.

Table 1.

Effect of 2-PAM on VX-induced acetylcholinesterase inhibition in frog sartorius muscle[a]

Treatment	Acetylcholinesterase activity (pmol/μg prot/min)	Enzyme inhibition (% control)
Control	5.55 ± 0.24	0
VX 20 μM	2.25 ± 0.13	60
VX 20 μM and:		
2-PAM 100 μM	2.14 ± 0.16	61
2-PAM 500 μM	2.13 ± 0.08	62
2-PAM 2 mM	3.12 ± 0.35	44

[a] Acetylcholinesterase activity was determined by the method of Ellman et al. (19).

Note the absence of reactivation of acetylcholinesterase with 100-500 μM 2-PAM. About 16% reactivation was noted with 2 mM 2-PAM.

Table 2.

Influence of pretreatment with carbamates
on subjunctional lesions induced by a lethal dose of sarin

Groups	Number of endplates/ Rats	Subjunctional Lesion Area (μM^2)	Perimeter (μM)	Length (μM)	Width (μM)
Untreated[a]	40/3	124 ± 8	72 ± 3	27 ± 2	10 ± 1
Sarin 1 hr[b]	49/3	2018 ± 163	206 ± 12	64 ± 4	46 ± 3
Sarin 5 days	93/3	493 ± 47	122 ± 7	41 ± 2	20 ± 1
Sarin 10 days	34/3	221 ± 25	94 ± 8	33 ± 3	12 ± 1
(+) physostigmine [(+)PHY]					
(+)PHY 1 hr[d]	40/3	183 ± 20	74 ± 3	29 ± 3	10 ± 1
(+)PHY-sarin 1 hr[d]	35/3	289 ± 19[c]	90 ± 3[c]	34 ± 2[c]	12 ± 1[c]
(+)PHY-sarin 5 days	32/3	indistinguishable from normal controls			
(-) physostigmine [(-)PHY]					
(-)PHY 1 hr[e]	48/4	228 ± 24	76 ± 3	29 ± 3	10 ± 1
(-)PHY-sarin 1 hr[e]	101/4	273 ± 15[c]	89 ± 3[c]	29 ± 1[c]	12 ± 1[c]
(-)PHY-sarin 5 days	93/3	indistinguishable from normal controls			

a. These values for the size of the endplate sarcoplasm are taken from a series of untreated in vivo muscles. The comparison is meant to provide general guidance.

b. The animals were injected with a subcutaneous dose of sarin (0.08 mg/kg) and sacrificed 1 hr, 5 days and 10 days later for morphological studies;

c. The values for (+)PHY (0.3 mg/kg) pretreatment prior to a lethal dose of sarin (0.13 mg/kg) were significantly smaller than those observed after a sublethal dose sarin (0.80 mg/kg) alone, $P<0.001$. Similarly significant differences were found when (-)physostigmine was used.

d. The animals were either injected with (+)PHY (0.3 mg/kg) alone and sacrificed 1 hr later or pretreated with this dose for 30 min before injection of a lethal dose of sarin (0.13 mg/kg) and sacrificed 1 hr later or at day 5;

e. The sequence of treatment was the same as in the previous group, except the drug used was (-)PHY (0.1 mg/kg).

E. Reference List:

1. Takeuchi, A., and Takeuchi, N. Active phase of frog's end-plate potential. J. Physiol. (Lond.) 22:395-411, 1959.

2. Kuba, K., Albuquerque, E.X., Daly, J., and Barnard, E.A. A study of the irreversible cholinesterase inhibitor, diisopropylfluorophosphate, on time course of end-plate currents in frog sartorius muscle. J. Pharmacol. Exp. Ther. 189:499-512, 1974.

3. Masukawa, L.M., and Albuquerque, E.X. Voltage- and time-dependent action of histrionicotoxin on the endplate current of the frog muscle. J. Gen. Physiol. 72:351-367, 1978.

4. Anderson, R., and Stevens, C.F. Voltage clamp analysis of acetylcholine produced end-plate current fluctuations at frog neuromuscular junction. J. Physiol. (Lond.) 235:655-691, 1973.

5. Adler, M., Oliveira, A.C., Albuquerque, E.X., Mansour, N.A., and Eldefrawi, A.T. Reaction of tetraethylammonium with the open and closed conformations of the acetylcholine receptor ionic channel complex. J. Gen. Physiol. 74:129-152, 1979.

6. Maleque, M.A., Souccar, C., Cohen, J.B., and Albuquerque, E.X. Meproadifen reaction with the ionic channel of the acetylcholine receptor: potentiation of agonist-induced desensitization of the frog neuromuscular junction. Mol. Pharmacol. 22:636-647, 1982.

7. Hamill, O.P., Marty, A., Neher, E., Sakmann, B., and Sigworth, F.J. Improved patch clamp techniques for high-resolution current recording from cells and cell-free membrane patches. Pflügers Arch. 391:85-100, 1981.

8. Allen, C.N., Akaike, A., and Albuquerque, E.X. The frog interosseal muscle fiber as a new model for patch clamp studies of chemosensitive and voltage-sensitive ion channels: actions of acetylcholine and batrachotoxin. J. Physiol. (Paris) 79:338-343, 1984.

9. Sachs, F., Neil, J., and Barkakati, N. The automated analysis of data from single ion channels. Pflügers Arch. Eur. J. Physiol. 395:331-340, 1982.

10. Meshul, C.K., Boyne, A.F., Deshpande, S.S., and Albuquerque, E.X. Comparison of the ultrastructural myopathy induced by anticholinesterase agents at the endplate of rat soleus and extensor muscles. Exp. Neurol. 89:96-114, 1985.

11. Karnovsky, M.J., and Roots, L. A direct coloring thiocholine method for cholinesterase. J. Histochem. Cytochem. 12:219-221, 1964.

12. Aracava, Y., Deshpande, S.S., Rickett, D.L., Brossi, A., Schönenberger, B., and Albuquerque, E.X. Molecular basis of anticholinesterase

actions on the nicotinic and glutamatergic synapses. Ann. N.Y. Acad. Sci. (in press).

13. Albuquerque, E.X., Deshpande, S.S., Aracava, Y., Alkondon, M., and Daly, J.W. (1986) A possible involvement of cyclic AMP in the expression of desensitization of the nicotinic acetylcholine receptor. A study with forskolin and its analogs. FEBS Lett. 199:113-120.

14. Huganir, R.L., Delcour, A.H., Greengard, P., and Hess, G.P. (1986) Phosphorylation of the nicotinic acetylcholine receptor regulates its rate of desensitization. Nature (Lond.) 321:774-776.

15. Middleton, P., Jaramillo, F., and Schuetze, S.M. (1986) Forskolin increases the rate of acetylcholine receptor desensitization at rat soleus endplates. Proc. Natl. Acad. Sci. USA 83:4967-4971.

16. Shaw, K.-P., Aracava, Y., Akaike, A., Daly, J.W., Rickett, D.L., and Albuquerque, E.X. (1985) The reversible cholinesterase inhibitor physostigmine has channel-blocking and agonist effects on the acetylcholine receptor-ion channel complex. Mol. Pharmacol. 28:527-538.

17. Varanda, W.A., Aracava, Y., Sherby, S.M., Vanmeter, W.G., Eldefrawi, M.E., and Albuquerque, E.X. (1985) The acetylcholine receptor of the neuromuscular junction recognizes mecamylamine as a noncompetitive antagonist. Mol. Pharmacol. 28:128-137.

18. Albuquerque, E.X., Deshpande, S.S., Kawabuchi, M., Aracava, Y., Idriss, M., Rickett, D.L., and Boyne, A.F. (1985) Multiple actions of anticholinesterase agents on chemosensitive synapses: Molecular basis for prophylaxis and treatment of organophosphate poisoning. Fund. Appl. Toxicol. 5:S182-S203.

19. Ellman, G.L., Courtney, K.D., Andres, V., Jr., and Featherstone, R.M. A new and rapid colorimetric determination of acetylcholinesterase activity. Biochem. Pharmacol. 7:88-95, 1961.

Distribution list:

1 copy Commander
US Army Medical Research and Development Command
ATTN: SGRD-RMI-S
Fort Detrick, Frederick, Maryland 21701-5012

5 copies Commander
US Army Medical Research and Development Command
ATTN: SGRD-PLE
Fort Detrick, Frederick, Maryland 21701-5012

2 copies Defense Technical Information Center (DTIC)
ATTN: DTIC-DDAC
Cameron Station
Alexandria, VA 22304-6145

1 copy Dean
School of Medicine
Uniformed Services University of the
Health Sciences
4301 Jones Bridge Road
Bethesda, MD 20814-4799

1 copy Commandant
Academy of Health Sciences, US Army
ATTN: AHS-CDM
Fort Sam Houston, TX 78234-6100